

Cite as: Liu P., Lei B., Huang W., Biljecki, F., Wang Y., Li, S., and Stouffs, R. (2025): Sensing climate justice: A multi-hyper graph approach for classifying urban heat and flood vulnerability through street view imagery. *Sustainable Cities and Society*, 118: 106016.

# Sensing Climate Justice: A Multi-Hyper Graph Approach for Classifying Urban Heat and Flood Vulnerability through Street View Imagery

Pengyuan Liu<sup>a</sup>, Binyu Lei<sup>b</sup>, Weiming Huang<sup>c</sup>, Filip Biljecki<sup>b,d</sup>, Yuan Wang<sup>b</sup>, Siyu Li<sup>b</sup>, Rudi Stouffs<sup>b</sup>

<sup>a</sup>*Future Cities Lab Global, Singapore-ETH Centre, Singapore*

<sup>b</sup>*Department of Architecture, National University of Singapore, Singapore*

<sup>c</sup>*Department of Physical Geography and Ecosystem Science, Lund University, Sweden*

<sup>d</sup>*Department of Real Estate, National University of Singapore, Singapore*

---

## Abstract

Recognising the increasing complexities posed by climate challenges to urban environments, it is crucial to develop holistic capabilities for urban areas to effectively respond to climate-related risks, forming the backbone of sustainable urban planning strategies and demanding a comprehensive understanding of urban climate justice. It requires a thorough examination of how climate change exacerbates social, economic, and environmental inequalities within urban settings, which requires a series of sophisticated spatial modellings and relies on data collected periodically. This paper introduces a novel dual-GNN approach, Multi-Hyper Graph Neural Network (MHGNN), with street view imagery as input. The proposed model integrates a multigraph and a hypergraph to model intricate spatial patterns for classifying urban climate justice. The multigraph component of the MHGNN captures spatial proximity and pair-wise connections between urban areas to assess climate impacts. Meanwhile, the hypergraph component addresses higher-order dependencies

by incorporating hyperedges that connect multiple geographic areas based on their similarities, thus capturing the multi-faceted relationships among areas with comparable geographic characteristics. By harnessing the strengths of both multigraph and hypergraph structures, the MHGNN provides a comprehensive understanding of the spatial dynamics of urban climate justice. It achieves nearly a 24% performance improvement compared to conventional spatial modelling methods, establishing it as a valuable tool for researchers and policymakers in this domain. Codes available at GitHub<sup>1</sup>.

*Keywords:* Spatial Modelling, Graph Neural Network, Multigraph, Hypergraph, Urban Resilience

---

## 1. Introduction

Cities are home to human habitation, housing a major proportion of the global population, economic activity, and critical physical infrastructure. However, urban areas, especially in the past decades, are increasingly vulnerable to the impacts of climate change, which is projected to intensify the frequency and severity of flooding, heat waves, droughts, and other hazardous events (Tuholske et al., 2021; Lankao and Qin, 2011). However, urban areas react to natural hazards in diverse ways; for instance, coastal cities may implement seawalls and storm surge barriers to combat flooding, while cities in hot climates can establish green roofs and urban forests to mitigate the effects of heatwaves. Such measurements often reflect the unique socio-economic, environmental, and infrastructural characteristics of each city and different areas within (Sultana, 2022; Porter et al., 2020; Schlosberg and Collins, 2014),

---

<sup>1</sup><https://github.com/anonymized-for-review>

leading to consequences that some people and places are more exposed to the direct impacts of climate change due to their location but with less capacity to respond. Hence, the disparity in exposure and the unequal capacity to respond to climate change underscore the urgent need for a holistic understanding of urban climate justice (Sebestyen et al., 2023; Steele et al., 2015; Broto and Bulkeley, 2013).

Understanding urban climate justice involves examining how climate change exacerbates social, economic, and environmental inequities in urban settings (Shi et al., 2016), seeking to identify who is most affected by climate change impacts and why, considering factors such as socio-economic status, race, ethnicity, and geographic location (Surminski et al., 2020). The concept extends beyond mere vulnerability assessment; it calls for transformative actions that promote fairness and equity in both mitigating climate change and adapting to its inevitable consequences. Census statistics and remote sensing images are often the most common data sources to study urban climate justice (Amorim-Maia et al., 2022). One of the examples of using census statistics to understand urban climate justice is the project *Climate Just* (Sayers et al., 2017; Lindley et al., 2014), which was initiated in 2014 in the United Kingdom (UK) to address the intertwined relationship between climate change and social justice. While census statistics are valuable for analysing complex patterns of human-urban interactions, they represent a periodic snapshot (e.g., every decade in the UK) that remains fixed in a rapidly changing world (Coleman, 2013). Remote sensing, on the other hand, offers the bird's eye view of the Earth's surface with more frequent data collection and has been widely used for environmental-related research

(Weigand et al., 2019). However, remote sensing satellites often provide data at resolutions that may not be fine enough to capture detailed urban features or small-scale variations within cities (Cao and Lam, 2023), putting barriers for the specific urban micro-climates, such as small parks or individual streets. Therefore, it is hard to analyse urban climate justice at a fine scale (e.g., street or neighbourhood level) with remote sensing images.

Recently, street view imagery (SVI) has emerged as a valuable data source for studying urban environments (Biljecki and Ito, 2021), unlocking new potential for human-eye-level understanding of urban characteristics (Ito et al., 2024) at a fine spatial resolution in quantitative analysis of environmental urban justices, such as urban greenery (Lu et al., 2023; Xia et al., 2021; Li et al., 2015b), pollution (Nathvani et al., 2023; Qi and Hankey, 2021; Apte et al., 2017), and living quality (Rui and Cheng, 2023; Yin et al., 2023). Most research utilises imagery from Google Street View (GSV) for urban analytics (Biljecki and Ito, 2021); however, crowdsourcing SVIs from platforms like Mapillary and KartaView provides broader spatial coverage, capturing images from virtually any location in the city, which has attracted increasing interest from experts in the field (Huang et al., 2024; Biljecki et al., 2023). To support the use of SVIs in urban analytics, image segmentation—a computer vision technique that partitions a digital image into discrete groups of pixels for object detection and related tasks—alongside a wide range of geospatial artificial intelligence (GeoAI) methods, has been developed for quantitative urban sensing (Zhang et al., 2024a).

GeoAI, integrating AI methods into spatial analytics, has been a trending technique in urban studies (Wang et al., 2024; De Sabbata et al., 2023b;

Liu and Biljecki, 2022). Graph Neural Networks (GNNs) are a set of AI methods using graph modelling of geospatial phenomena and are capable of encapsulating the spatial relationships among geospatial objects into the computational process (Mai et al., 2022). Hence, GNNs are widely acknowledged as a genre of spatially-explicit GeoAI methods (Liu and Biljecki, 2022). To facilitate GNNs in urban analytics, it is often a common practice to use graphs to represent street networks (i.e., connectivity) with aggregated SVI segmentation as streets' features for downstream tasks (Ma et al., 2024; Liu et al., 2024; De Sabbata et al., 2023a; Zhang et al., 2023). GNNs, then, consider Tobler's First Law of Geography (Tobler, 1970) by leveraging spatial proximity and relational dependencies among nodes, incorporating spatial information through graph structures, where geographically closer nodes often have stronger connections, leading to more influence during message passing.

Despite its usefulness in various urban analytical tasks (Liu and Biljecki, 2022), such a naive way of spatial modelling overlooks the high-order latent interactions among spatial areas, failing to account for the attribute similarity between locations that may exhibit highly correlated relationships even across more distant locations (Wang and Zhu, 2024; Zhu et al., 2018). Such high-order spatial interaction often refers to the Third Law of Geography (Zhu and Turner, 2022; Zhu et al., 2018), which is particularly interesting for studying urban climate justice context, highlighting how similar socio-environmental conditions can drive interactions and inequalities, informing more equitable climate policies and interventions. However, for spatially-explicit GeoAI development, incorporating the Third Law of Geography remains an underexplored research direction in current GNN-based GeoAI de-

velopment.

This paper proposes a dual GNN-based analytical framework, Multi-Hyper Graph Neural Network (MHGNN), combining a hypergraph-based GNN and a multigraph-based GNN to classify urban climate justice, focusing on flooding and heat resilience using SVIs from Mapillary. The hypergraph-based GNN captures high-order, attribute-based relationships among distant but similar areas, effectively incorporating the Third Law of Geography. For example, in a large city, consider three urban areas—Area A, Area B, and Area C—that, while geographically dispersed, share similar socio-economic vulnerabilities such as high population densities, low incomes, and minimal green spaces, making them particularly susceptible to heatwaves. A hypergraph model effectively connects these areas not through geographic proximity but via a hyperedge that represents their shared characteristics, allowing for comprehensive analysis and targeted climate resilience interventions, such as coordinated cooling centres, despite the areas not being physically adjacent, thus enhancing urban planning and adaptation strategies in a way traditional graphs could not. Meanwhile, the multigraph-based GNN still understands spatial proximity and pair-wise direct connections among geographically closer areas, adhering to the First Law of Geography. We demonstrate that such a dual-graph-based approach incorporating both the first and the third laws of geography ensures a comprehensive spatial analysis of the urban environment by considering spatial and attribute similarities across urban regions.

To provide an overview of this study and its contributions, in this paper:

- we advance the technological advancement in urban justice studies at

a fine spatial resolution by proposing a dual GNN-based analytical framework, which incorporates both the First and the Third Law of Geography;

- we propose a new ground-breaking spatial modelling method, which captures both the high-order spatial interactions among areas that are distant from each other and also the pair-wise spatial connections between areas;
- we showcase the use of crowdsourced SVIs in urban analytical tasks, promoting the potential of volunteered geographic information (VGI) in urban studies.

## 2. Background and Related Work

### 2.1. Urban Climate Justice: Flooding and Heat Waves

Urban climate justice is an emerging field that examines the intersection of climate change impacts, social equity, and urban environments (Zhang et al., 2024b; Surminski et al., 2020; Shi et al., 2016), which recognises that the effects of rapid climate change in the past decades, such as flooding and extreme heat, are not experienced equally across different urban populations (Bulkeley et al., 2014). Such a disparity often exacerbates existing social inequalities, disproportionately affecting vulnerable communities with the least capacity to adapt and respond to these challenges.

Flooding is one of the most pressing climate change impacts in urban areas (Dharmarathne et al., 2024; Wang et al., 2023; Chang and Huang, 2015; Schreider et al., 2000). Intense rainfall, sea level rise, and inadequate

drainage systems often lead to severe urban flooding, which can devastate local communities across cities (Latham et al., 2024; Mignot and Dewals, 2022). Meanwhile, flooding highlights significant social disparities. Due to historical housing practices and economic constraints, lower-income neighbourhoods are often situated in flood-prone areas with inadequate infrastructure, facing the brunt of flood-related damages (Zhu et al., 2021; Aroca-Jiménez et al., 2020). In the meantime, those neighbourhoods may suffer from long-term setbacks after flooding events because of insufficient financial resources or insurance coverage for the local residents to repair and rebuild after flood events (Wang et al., 2021).

Meanwhile, extreme heat is another critical aspect of urban climate justice. Urban areas, with their dense concentrations of buildings and infrastructure, often experience higher temperatures than their rural counterparts, a phenomenon known as the urban heat island effect (Kim and Brown, 2021). During heatwaves, such an effect can worsen the health risks for urban residents. Vulnerable populations, such as the elderly, children, pregnant women, and those with pre-existing health conditions, are particularly at risk due to physiological factors (Park et al., 2021; Ebi et al., 2021). Additionally, low-income communities lack access to cooling resources such as air conditioning, green spaces, and adequate healthcare, rendering them more susceptible to the adverse effects of extreme heat (Benz and Burney, 2021; Ebi et al., 2021). In densely populated urban areas, housing quality can also play a significant role; poorly insulated homes can trap heat, creating hazardous living conditions during heatwaves (Yadav et al., 2023).

Therefore, addressing urban climate justice involves integrating social eq-

uity into climate adaptation and mitigation strategies (Bulkeley et al., 2014), and having a holistic understanding of local socio-economic status to react to rapid climate changes is often the first step (Karanja and Kiage, 2021; Xu et al., 2021). As mentioned in the Introduction, the Climate Just project, initiated in 2014, is a groundbreaking initiative in the United Kingdom aimed at addressing the intersection between climate change and social justice to identify and mitigate the disproportionate impacts of climate change on vulnerable populations (Sayers et al., 2017; Lindley et al., 2014), with a particular focus on both flooding and heat waves. Based on 2011 UK census statistics, the project developed comprehensive indices to measure socio-economic vulnerabilities within urban populations in handling, adapting, and recovering from floods or urban heat waves, or both (Lindley et al., 2014). Such indices served as a critical resource for local authorities, urban planners, and community organisations, providing a robust evidence base for prioritising investments and interventions that enhance climate resilience in a socially equitable manner. Our study takes the indices developed by Climate Just not only as a proxy to understand neighbourhood-level urban resilience but also as ground-truth data to train our proposed dual GNN-based analytical framework (see Section 4).

## *2.2. Street View Images: Quantitative Measurement of Urban Environment*

The advent of SVI has revolutionised the quantitative analysis of urban environments (Ito et al., 2024; Zhang et al., 2024a; Biljecki and Ito, 2021). Early applications of SVIs in urban studies focused primarily on visual assessments of urban landscapes. Researchers utilised these images for qualitative evaluations, such as assessing streetscape aesthetics, pedestrian

infrastructure, and urban greenery (Ben-Joseph et al., 2013; Rundle et al., 2011). In recent years, machine learning and computer vision techniques have since facilitated a shift towards more quantitative approaches. Convolutional Neural Networks (CNNs) and their further applications in image recognition algorithms, such as object detection and image segmentation, have been employed to automate the extraction of urban features from SVIs, enabling large-scale and objective measurements (Biljecki and Ito, 2021), opening up new potentials in studying urban environmental justice (Lu and Chen, 2024).

One prominent application of SVIs is the quantification of urban greenery, shading structures, and reflective surfaces Biljecki et al. (2023); Yang et al. (2023), which are crucial in mitigating the urban heat island effect (Price et al., 2015). For example, Li et al. (2015a) developed a methodology using GSVs to measure the Green View Index (GVI), which quantifies the visible green space from the street level. Their proposed method accurately represents human exposure to greenery compared to traditional aerial or satellite imagery. By analysing the distribution of green spaces, researchers can identify areas lacking adequate greenery, often corresponding to lower-income neighbourhoods, thus highlighting issues of environmental inequality (Cheng et al., 2024). Meanwhile, research such as Li and Ratti (2019) proposed a method of solar radiation estimation at the street level based on the built environment structures identified using SVIs, offering new potential for better urban planning strategies facing the increasingly prolonged urban heat weaves throughout the years.

Other than the urban heat waves studies, SVIs offer a unique perspective for evaluating flood risk and resilience at the street level, assessing the con-

dition and capacity of drainage systems (Boller et al., 2019), the prevalence of permeable surfaces (Kim et al., 2022), and the presence of flood defences (Percival et al., 2020). Mapping urban flood facilities through SVIs allows policymakers to understand urban flooding vulnerabilities (Koks et al., 2015), prioritising investments in flood resilience where they are most needed and ensuring necessary interventions are socially equitable (Tyler et al., 2023; Hofflinger et al., 2019).

Inspired by the recent trend of using SVIs to study urban environments, our study uses information identified and extracted from street-level images as the primary input for the proposed framework, developing a new GeoAI method and promoting the use of SVIs in intelligent urban environment understanding.

### *2.3. Spatially-explicit GeoAI: Laws of Geography*

Despite our study focusing on urban climate justice, our proposed method is inspired by a recent publication focusing on human activity intensity prediction (Wang and Zhu, 2024). In their research, the authors introduced a hypergraph-based hybrid graph convolutional network (HyGCN) for the spatiotemporal modelling of human activity intensity by incorporating both Tobler's First Law of Geography and the Third Law of Geography into the proposed spatial modelling task. The HyGCN model proposed in the article consists of three major components: a graph convolution layer (GCN), a hypergraph convolutional layer (HGCN) and a spatial fusion layer. The GCN layer was developed for capturing pair-wise relationships among areas, where each node updates its representation based on the features of its neighbours, mimicking the idea that the characteristics of a place are influenced

by nearby places, with the influence weighted by the distance or strength of the relationship; hence, effectively incorporating Tobler’s First Law of Geography in the model. Meanwhile, HGCN, as an underexplored GNN method in spatial analytical tasks, has been introduced in their paper to incorporate the Third Law of Geography. HGCN uses hyperedges to capture the high-order relationships among multiple locations based on the similarity of their geographic settings. That is, each node can have attributes that describe its geographic features, such as the intensity of human activities in their paper. Hyperedges, which connect multiple nodes, can represent the level of similarity among these locations, effectively illustrating how geographically similar areas tend to exhibit similar phenomena, adhering to the Third Law of Geography. After capturing the pair-wise and high-order relationship features produced by GCN and HGCN, a spatial fusion layer was implemented to capture the coupled nature of geographic relationships, where pair-wise relationships influence high-order relationships and vice versa, contributing to an enhanced prediction of human activity intensity.

Wang and Zhu (2024) serves as a fundamental inspiration for our proposed method. However, their method is relatively naive because both the pair-wise connections and the hypergraphs constructed for the population intensity studies focus only on the limited sets of spatialities in the model. In comparison, urban climate justice presents a more complex challenge involving the multifaceted nature of both environmental factors and socio-economic drivers (Shi et al., 2016). Consequently, we extended their method, tailoring the model to address various aspects of human-environmental interactions through intricate spatial modelling. Details of these modifications will be in-

troduced in Section 3. Nonetheless, the concept of incorporating both pairwise and high-order interactions among geographic areas provides us with unique insights into how a comprehensive understanding of spatial modelling contributes to a better understanding of the urban environment.

### 3. A Multi-Hyper Graph Neural Network for Urban Sensing

This study introduces a multifaceted approach to studying the urban environment and inferring urban climate justice through visual sensing and advanced machine learning techniques, as shown in Figure 1. We formalise the classification of urban climate justice as a semi-supervised learning task, outputting the levels of urban neighbourhoods’ resilience facing the risks of flooding, heatwaves, and both. The proposed method consists of four essential components: visual understanding of the urban environment, spatial-aware graph and high-order relationship graph modelling, and the MHGNN. In the following sections, we will provide a detailed introduction to each component and explain how they are integrated to enhance our understanding of urban climate justice.

#### 3.1. Visual Understanding of Urban Environment

As previously mentioned, the unequal distribution of the urban physical environment is often considered a key factor contributing to urban climate injustice, revealing disparities in environmental quality and access to resources across different urban areas (Surminski et al., 2020; Shi et al., 2016). Such inequity can lead to adverse health and socio-economic outcomes for marginalised communities, as well as their capabilities to respond to urban

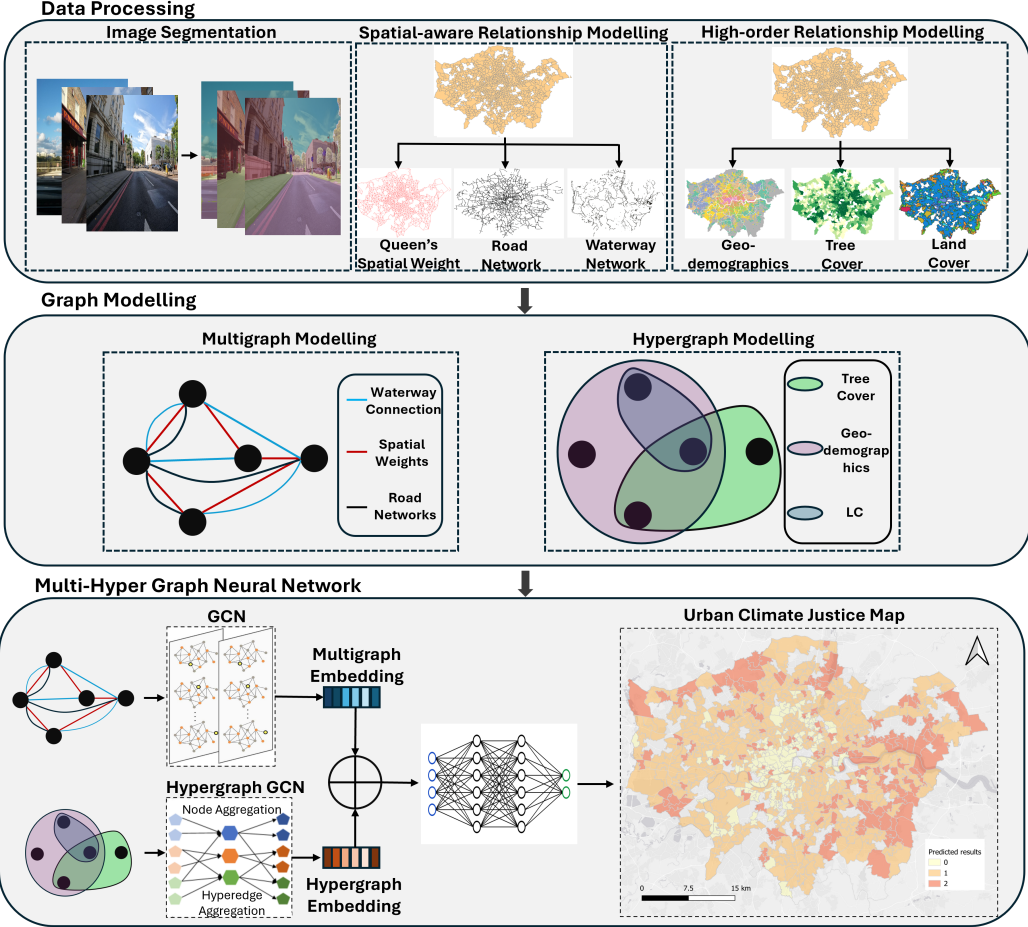


Figure 1: The overview of the proposed method. This figure includes SVIs obtained from Mapillary under the Creative Commons (CC) licence and the road network under the Open Government Licence. Map data source: CDRC LOAC Geodata Pack by the ESRC Consumer Data Research Centre; contains National Statistics data Crown copyright and database right 2015; contains Ordnance Survey data Crown copyright and database right 2015.

climate-related risks. In recent years, the rapid advancement of computer vision technologies has made image segmentation of SVIs a standard practice in urban analytics (Zhang et al., 2024a; Ito et al., 2024; Biljecki and Ito, 2021),

which provides a systematic and quantitative understanding of the proportion and distribution of urban objects in visual data, thereby supporting an in-situ comprehension of the urban physical environment.

In our study, we employed DeepLabv3 (Chen et al., 2017) to segment each image obtained from Mapillary and determine the percentages of various spatial objects in each SVI. DeepLabv3 was pre-trained on the CityScape dataset (Cordts et al., 2016) using PaddleSeg (Liu et al., 2021; PaddlePaddle Authors, 2019). The CityScape dataset, designed for the semantic understanding of urban street scenes, classifies 30 categories of urban objects in SVIs (Cordts et al., 2016). In our study, we utilised all 30 categories of urban objects segmented by DeepLabv3, facilitating a holistic understanding of the urban built environment. Therefore, for each neighbourhood (see Section 4 on the case study) within the city, we segmented all SVIs within its boundaries and calculated the mean values of each urban object category. These processed values were then used as input for the graph modelling introduced in the following sections.

### *3.2. Spatial-aware Graph Construction*

In recent years, conceptualising urban physical environments as graphs for the spatially-explicit development of GeoAI has become increasingly common (Liu and Biljecki, 2022). Such an innovative approach, effectively incorporating Tobler’s First Law of Geography in the model, allows for a more nuanced understanding of spatial relationships and interactions within urban areas. A prevalent method involves constructing spatial graphs based on physical connections that interlink urban neighbourhoods, such as street networks (Liu et al., 2024; Zhang et al., 2023; De Sabbata et al., 2023a), transporta-

tion routes (Rahmani et al., 2023), or spatial weights (De Sabbata and Liu, 2023). Researchers can facilitate pair-wise spatially aware graph construction by representing these connections as graph edges, with nodes corresponding to various urban elements or locations, enabling detailed analysis of spatial dependencies and influences, which are crucial for applications in urban environmental monitoring (Ma et al., 2023). However, existing methods of constructing such graphs often focus on a single spatial modality, such as the pair-wise graph constructed in Wang and Zhu (2024), relying on one type of spatial connection to study complex urban issues. This approach, while useful, can be limiting as it typically considers only one aspect of the urban environment (e.g., street networks) without integrating other critical spatial dimensions. Consequently, this single-modality focus may overlook the multifaceted interactions and dependencies that characterise urban systems, potentially leading to an incomplete understanding of the urban environment.

To address this issue, our research proposes a multigraph modelling approach to capture the pair-wise connections among urban neighbourhoods, aiming for a more comprehensive understanding of the urban environment. This innovative approach involves constructing multiple graphs, each representing different spatial modalities and interactions within the urban fabric. As shown in Figure 2, by integrating various dimensions such as road networks that interlink urban areas, queen contiguity spatial weights among neighbourhoods, and waterways throughout the city, our multigraph model provides a comprehensive representation of the urban environment.

Queen contiguity spatial weights are a widely-used method in spatial analysis that considers neighbourhoods to be adjacent if they share a com-

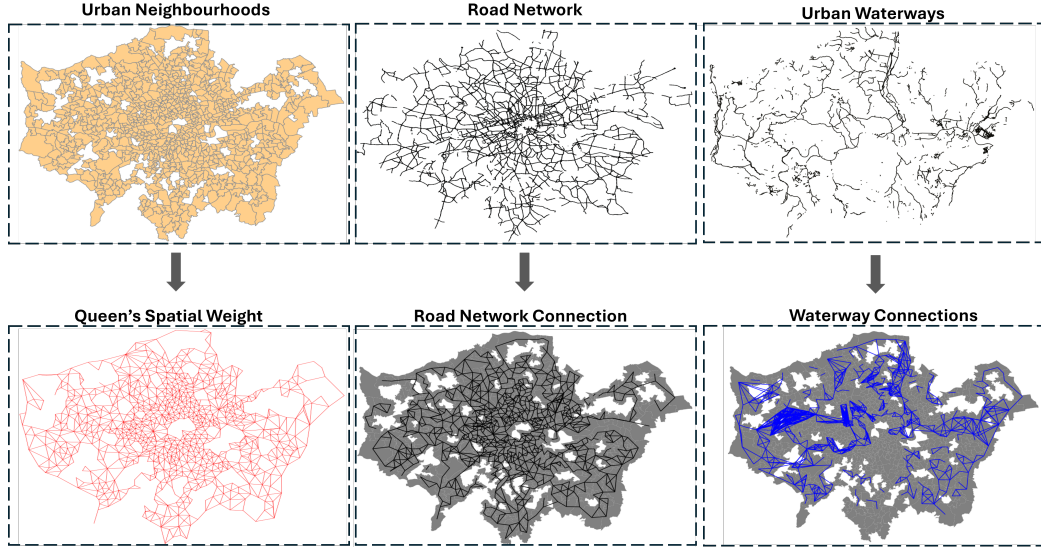


Figure 2: Spatial-aware Graph Construction. Detailed introduction about the data is provided in Section 4.

mon boundary or vertex. By applying this approach, we constructed a graph where nodes represent neighbourhoods and edges represent spatial contiguity, capturing the direct spatial relationships and dependencies among urban areas. Such an aspect of the multigraph helps in understanding how the proximity of neighbourhoods influences the classification of urban climate justice. The following equation shows how its adjacency matrix was represented:

$$A_{\text{Queen}}(i, j) = \begin{cases} 1 & \text{if neighbourhoods } i \text{ and } j \text{ are adjacent} \\ 0 & \text{otherwise} \end{cases} \quad (1)$$

In addition to queen contiguity spatial weights, we incorporated the city’s waterways into our multigraph model. Waterways, including rivers, canals, and streams, play a crucial role in shaping the urban environment (Luo

et al., 2022), cooling down cities (Park et al., 2019) and influencing the urban flooding risks (Rubinato et al., 2019). As shown in Figure 2, if two neighbourhoods have a waterway crossing through, an edge was added to the graph. The adjacency matrix for the urban waterway connections is as follows:

$$A_{\text{Water}}(i, j) = \begin{cases} 1 & \text{if a waterway connects neighbourhoods } i \text{ and } j \\ 0 & \text{otherwise} \end{cases} \quad (2)$$

Furthermore, we included the road networks within the city as another critical layer in our multigraph model. In the context of urban climate justice, road networks are fundamental to urban infrastructure, affecting the accessibility of neighbourhoods to relevant facilities when hazards happen (Dalziell and Nicholson, 2001). Similar to the process we implemented for the waterways, if two neighbourhoods have a road network across, an edge was added to the graph. Similar to the waterway connections, the adjacency matrix for the urban road network connections is:

$$A_{\text{Road}}(i, j) = \begin{cases} 1 & \text{if a road connects neighbourhoods } i \text{ and } j \\ 0 & \text{otherwise} \end{cases} \quad (3)$$

Having the adjacency matrices  $A_{\text{Queen}}$ ,  $A_{\text{Water}}$ , and  $A_{\text{Road}}$ , we defined the combined adjacency matrix for the multigraph as:

$$A_{\text{Multi}} = A_{\text{Queen}} + A_{\text{Water}} + A_{\text{Road}} \quad (4)$$

Integrating these three modalities—queen contiguity spatial weights, waterways, and road networks—allows our multigraph model to comprehensively represent the urban environment. In our research, we investigated how such a tri-layered approach facilitates the analysis of interactions and influences among different spatial elements, providing a more nuanced understanding of urban systems and, hence, assisting in better classification of urban climate justice.

### *3.3. High-order Relationship Graph Construction*

High-order relationships in spatial data refer to interactions and dependencies that extend beyond simple pair-wise connections between spatial entities. Unlike traditional spatial analyses that focus on direct, pair-wise relationships, high-order relationships capture the complex interactions among groups or clusters of entities. Hypergraphs, with their ability to represent complex, multi-way interactions among entities, offer significant opportunities for modelling these intricate spatial relationships in urban analytics (Wang and Zhu, 2024), echoing the Third Law of Geography (Zhu and Turner, 2022). Unlike the hypergraphs implemented in Wang and Zhu (2024), which focused on a single aspect of urban configurations (i.e., urban functions), our study extends the application of hypergraphs by incorporating a comprehensive understanding of urban environments, including socio-economic factors and environmental settings.

We constructed a hypergraph based on three data types: urban geodemographics, land cover data, and levels of tree coverage in the city (see Section 4 for details of the data), as shown in Figure 1. Having sets of categories for the three data types defined as  $C_{\text{demo}} = \{c_{\text{demo}_1}, c_{\text{demo}_2}, \dots, c_{\text{demo}_k}\}$  (for

geodemographics),  $C_{lc} = \{c_{lc_1}, c_{lc_2}, \dots, c_{lc_k}\}$  (for land cover), and  $C_{tree} = \{c_{tree_1}, c_{tree_2}, \dots, c_{tree_k}\}$  (for tree coverage), for each neighbourhood  $i$  in the urban area that is represented as a node  $v_i$ , we define indicator functions  $\delta_{demo}$ ,  $\delta_{lc}$ , and  $\delta_{tree}$  to determine whether a neighbourhood belongs to a specific category as:

$$\delta_{demo}(v_i, c_{demo_j}) = \begin{cases} 1 & \text{if } v_i \text{ belongs to } c_{demo_j} \\ 0 & \text{otherwise} \end{cases} \quad (5)$$

$$\delta_{lc}(v_i, c_{lc_j}) = \begin{cases} 1 & \text{if } v_i \text{ belongs to } c_{lc_j} \\ 0 & \text{otherwise} \end{cases} \quad (6)$$

$$\delta_{tree}(v_i, c_{tree_j}) = \begin{cases} 1 & \text{if } v_i \text{ belongs to } c_{tree_j} \\ 0 & \text{otherwise} \end{cases} \quad (7)$$

After completing the above steps, for each category, we created a hyper-edge connecting all neighbourhoods that share the same category:

$$e_{demo_j} = \{v_i \in V \mid \delta_{demo}(v_i, c_{demo_j}) = 1\} \quad (8)$$

$$e_{lc_j} = \{v_i \in V \mid \delta_{lc}(v_i, c_{lc_j}) = 1\} \quad (9)$$

$$e_{tree_j} = \{v_i \in V \mid \delta_{tree}(v_i, c_{tree_j}) = 1\} \quad (10)$$

Hence, in our study, the hypergraph  $H$  is defined as  $H = (V, E)$ , where  $V$  is the set of nodes and  $E$  is the set of hyperedges, and the hyperedges  $E$  include all hyperedges from the three categories:

$$E = \{e_{\text{demo}_1}, \dots, e_{\text{demo}_k}, e_{\text{lc}_1}, \dots, e_{\text{lc}_m}, e_{\text{tree}_1}, \dots, e_{\text{tree}_n}\} \quad (11)$$

Then, we represent the hypergraph  $H$  by using an incidence matrix  $M$  based on the hyperedges constructed:

$$M_{(i,j)} = \begin{cases} 1 & \text{if node } v_i \text{ is in hyperedge } e_j \\ 0 & \text{otherwise} \end{cases} \quad (12)$$

Such a multi-faceted hypergraph construction approach allows for a more detailed analysis of urban systems, as it considers various factors that influence potential urban capabilities in handling urban climate-related risks, such as socio-economic characteristics, land use patterns, and environmental features. In our study, the constructed hypergraph, together with the multigraph introduced in Section 3.1, was used as input for the proposed MHGNN.

### 3.4. The Multi-Hyper Graph Neural Network

As shown in Figure 1, the proposed MHGNN has two major parts: a GCN layer for handling the constructed multigraph and an HGNC for processing the hypergraph. Such an integration leverages the strengths of both types of convolutions to capture both pair-wise and high-order relationships among nodes. The combined features are then passed through a series of fully connected layers, followed by a softmax layer for classification.

Having segmented SVIs as nodes' features for each neighbourhood in the city as  $x_i$ , and the combined adjacency matrix  $A_{\text{Multi}}$ , the GCN part applies convolution operations (Kipf and Welling, 2016) to the adjacency matrix.

The feature update rule for node  $v_i$  is:

$$Embed^{(l+1)} = \sigma \left( \sum_{i=1}^k \alpha_i \tilde{A}_{\text{Multi}}^{(i)} Embed^{(l)} W^{(l)} \right) \quad (13)$$

where  $\tilde{A}_{\text{Multi}}^{(i)}$  is the normalised adjacency matrix for the  $i$ -th criterion,  $\alpha_i$  are learnable weights,  $Embed^{(l)}$  represents the node features at layer  $l$ ,  $W^{(l)}$  are the learnable parameters, and  $\sigma$  is an activation function of ReLU (Nair and Hinton, 2010). The final output of the GCN part after  $L$  layer is  $Embed^{(L)}$ , containing the updated feature representations of the nodes, incorporating information from their immediate neighbours according to the multiple pairwise connections.

Meanwhile, HGCN (Bai et al., 2021) extends the traditional GCN by incorporating hyperedges that connect multiple nodes, enabling the network to capture complex interactions and dependencies among neighbourhoods. Having the hypergraph's incidence matrix  $M$  correspond to the incidence of nodes in the hyperedges, HGCN computes the hypergraph Laplacian  $Lap_i$  for the matrix:

$$Lap_i = I - D_v^{-1/2} M_i W M_i^T D_v^{-1/2} \quad (14)$$

where  $I$  is the identity matrix;  $D_v$  is the diagonal degree matrix of nodes;  $M_i$  is the incidence matrix for the  $i$ -th criterion;  $W$  is the diagonal matrix of hyperedge weights.

The convolution operation on the hypergraph uses the hypergraph Laplacian to propagate information across nodes (Bai et al., 2021), and the feature update rule is given by:

$$HEmbed^{(l+1)} = \sigma \left( \sum_{i=1}^k \beta_i Lap_i HEmbed^{(l)} W^{(l)} \right) \quad (15)$$

where  $H\text{Embed}^{(l)}$  is the feature matrix at layer  $l$ ;  $\beta_i$  are learnable weights for each hypergraph;  $Lap_i$  is the hypergraph Laplacian for the  $i$ -th criterion;  $W^{(l)}$  are learnable parameters;  $\sigma$  is an activation function of ReLU (Nair and Hinton, 2010). The output of HGNC is  $H\text{Embed}^{(L)}$ , containing the updated feature representations of the nodes, incorporating high-order relationships among nodes connected by hyperedges.

The output of GCN and HGNC is then concatenated to integrate pairwise and high-order relationships in the urban environment as:

$$Embed_{concat} = concat(Embed^{(L)}, H\text{Embed}^{(L)}) \quad (16)$$

which is then passed through fully connected layers and a softmax layer to produce the final classification scores:

$$Z = softmax(Embed_{concat}W_{final}) \quad (17)$$

where  $W_{final}$  are the learnable weights of the final layer. The model is trained using a supervised learning approach, where the cross-entropy loss measures the discrepancy between the predicted classifications and the true labels. The parameters of the network are optimised using backpropagation to minimise this loss:

$$\mathcal{L} = - \sum_{i=1}^n \sum_{j=1}^c y_{ij} \log(Z_{ij}) \quad (18)$$

where  $y_{ij}$  is the true label for node  $i$  and class  $j$ .

### 3.5. Model Implementation

We developed our proposed framework using the Python programming language, specifically utilising the PyTorch library (Paszke et al., 2019) and

the PyTorch Geometric library (Fey and Lenssen, 2019) for implementation. The model, known as the MHGNN, was fully trained over 2000 epochs for a semi-supervised classification task, with each epoch representing a complete pass through the dataset. The dataset was split into 30% for training, 10% for validation, and 60% for testing, and the training was conducted on the cloud-based Google Colab platform<sup>2</sup>. We employed the Adam optimisation algorithm (Kingma and Ba, 2014) with a learning rate of 0.001 to refine the model’s weights.

In line with standard practices for classification models, we selected accuracy and the F1 score (a metric that combines precision and recall into a single measure and evaluates the accuracy of the classification model by balancing the trade-off between false positives and false negatives) for the model’s performance assessment.

### *3.6. Benchmark Comparisons*

To evaluate the performance of MHGNN, we selected three prediction methods, ranging from classical to state-of-the-art, as benchmark comparisons for classifying overall urban sensitivity to both flooding and heat stress:

- Random Forest (RF) is recognised as one of the most classical machine learning models and is extensively utilised for various urban analytical tasks (Luo et al., 2022; Ameer and Shah, 2018; Puissant et al., 2014). In this assessment, RF serves as a non-spatial model, taking image segmentation results as input. It provides a baseline comparison to highlight the advantages of incorporating spatial data and connections,

---

<sup>2</sup><https://colab.research.google.com/>

as MHGNN does, in urban climate justice classification. The selection of RF is motivated by its robustness and popularity in urban studies (Lavallin and Downs, 2021), where non-spatial data alone have been used effectively for classification tasks. Such a comparison allows us to examine how spatial relationships improve prediction when compared to a traditional, non-spatial approach.

- GraphSAGE (Hamilton et al., 2017) is an inductive graph-based framework that generates node embeddings by sampling and aggregating features from a node’s local neighbourhood, which are not widely used in urban analytics (Zhang et al., 2022; Liu et al., 2023). GraphSAGE is included to compare MHGNN against another graph-based method that focuses on local neighbourhood information aggregation, thus allowing us to explore how different forms of graph representation influence classification performance. We adapted GraphSAGE to handle multigraph and hypergraph structures by integrating the two graphs’ adjacency matrices, which ensures a fair comparison between models while maintaining the graph-based focus. By including GraphSAGE, we assess MHGNN’s ability to effectively handle more complex graph structures.
- Deep Graph Infomax (DGI) (Veličković et al., 2019) is a graph representation learning technique that can serve as a benchmark for evaluating how well the proposed method captures graph structures and relationships. However, DGI is primarily designed for single graph structures with simple edges between nodes. To handle multigraphs and hypergraphs, we applied further modifications to accommodate

the complexities of these types of graphs. Similar to MHGNN, DGI in this study consists of two encoders to process the constructed multi-graph and hypergraph individually, a GCN (Kipf and Welling, 2016) encoder and a HGCN (Bai et al., 2021) encoder. The two encoders learnt the two graph structures separately in an unsupervised manner and output a joint embedding for the supervised fine-tuning climate justice classification task.

All three of the aforementioned benchmark methods are evaluated using two of the same performance metrics: accuracy and the F1 score, as mentioned in the previous subsection. The results of these evaluations, including detailed comparisons across models, are presented in Section 5, where we demonstrate how each method performs in comparison with MHGNN.

#### 4. Case Study

In this study, we have selected Greater London (shortened to *London* for the rest of this paper), UK, as our case study area. London offers a compelling case study for examining urban climate justice due to its diverse demographic composition, extensive urban infrastructure, and proactive climate policies (Bulkeley et al., 2013). As one of the world’s leading global cities, London is home to approximately nine million residents from varied socio-economic backgrounds, ethnicities, and cultures. While hosting such a significant number of residents within its urban area, the city faces numerous environmental challenges, including flooding and heatwaves, exacerbated by ever-complicated climate challenges (Keat et al., 2021). Being aware that

such challenges are not uniformly distributed across the city, with vulnerable neighbourhoods often experiencing disproportionate impacts, our study explored how spatially-explicit GeoAI-empowered methods can provide enhanced support for understanding urban resilience at a fine spatial resolution facing risks of climate hazards.

#### *4.1. London Climate Just Data*

As previously discussed in Section 2, the Climate Just project in London served as a fundamental inspiration for our study. Based on 2011 UK census statistics, this project systematically produced indices on urban socio-spatial vulnerability to flooding and heat stress separately, as well as a composite index on the overall urban sensitivity to both flooding and heat stress, as illustrated in the top three figures of Figure 3. Positive scores indicate increasing vulnerability and sensitivity, and vice versa. The data is available at the Middle Super Output Area (MSOA) level for London.

In the UK, MSOAs are considered a valuable unit for neighbourhood studies because they provide a standardised geographic framework for analysing social, economic, and health data at a granular level. MSOAs typically encompass populations between 5,000 and 15,000 people, making them large enough to capture meaningful statistical trends while being small enough to reflect local neighbourhood characteristics. Therefore, in our study, all analyses were conducted at the MSOA level in London to ensure detailed and reliable insights specific to neighbourhoods.

Additionally, as illustrated in Figure 3, we refined the indices from the Climate Just project by categorising them based on the Jenks classification method (Jenks, 1975) into three distinct classifications designated as low,

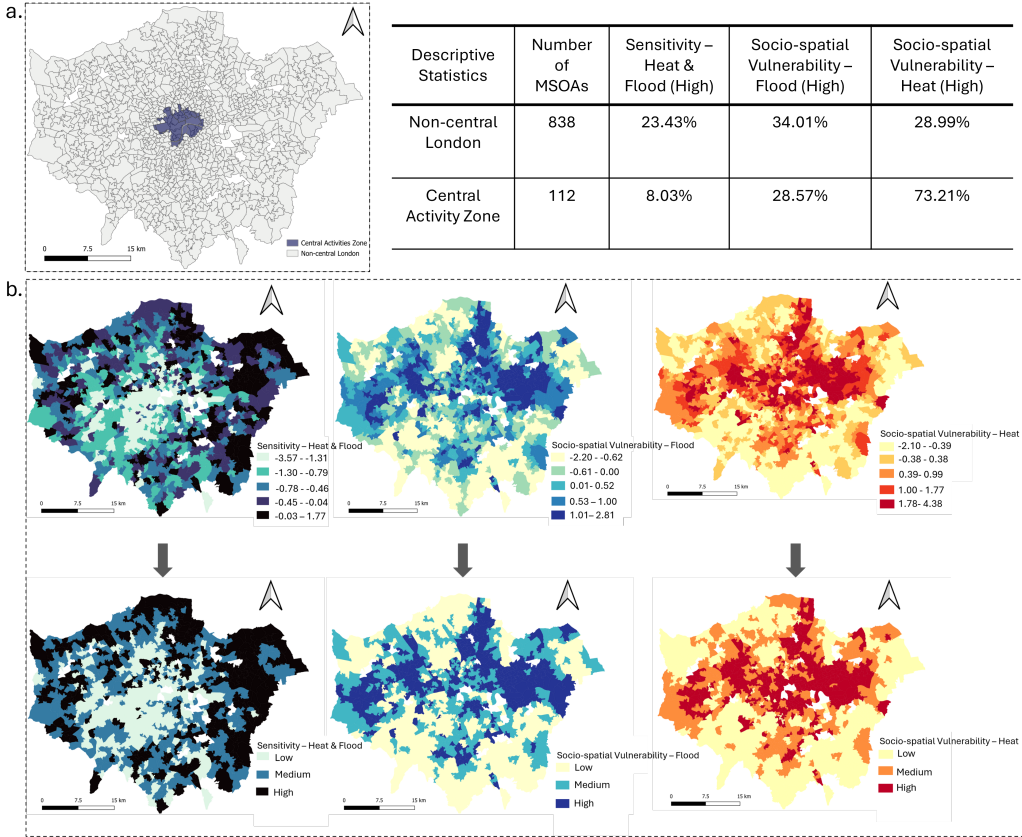


Figure 3: On the top left of the figure, a. demonstrates the city centre of London defined by the Central Activity Zone by Greater London Authority. In b., from top left to top right: Overall sensitivity index for both Flooding and Heat risks; Socio-spatial vulnerability index for flood; Socio-spatial vulnerability index for heat. From bottom left to bottom right: Three categorical classifications for the above indices. The missing parts in the maps are those MSOAs in London that had no Climate Just indices produced; hence, those neighbourhoods were excluded from this study. For Climate Just data, we have 950 MSOAs presented in the figure. Map data source: CDRC LOAC Geodata Pack by the ESRC Consumer Data Research Centre; contains National Statistics data Crown copyright and database right 2015; contains Ordnance Survey data Crown copyright and database right 2015.

medium, and high, to enhance the interpretability of the indices across London, thereby facilitating a clearer understanding and communication of the varying levels of climate vulnerability present within the city. The table in Figure 3 reveals that central London exhibits a significantly higher percentage of areas that face heat vulnerability compared to non-central areas, potentially due to a stronger urban heat island effect (Taylor et al., 2015). However, it shows more favourable conditions for flood vulnerability and overall urban sensitivity to both heat and flood risks thanks to its accessibility to urban facilities (Lamond et al., 2009). In our study, these classified indices were employed as ground truth labels, serving a critical role in the training and evaluation of our proposed GeoAI-driven classification method, ensuring that the identified areas accurately reflect real-world conditions, thereby enhancing the reliability of our method and the findings.

#### *4.2. Crowdsourcing Street View Imagery*

For the SVIs adopted as input for this study, we acquired data from Mapillary, covering the period from the 1<sup>st</sup> of January 2020 to the 22<sup>nd</sup> of September 2022 in London, resulting in the collection of 529,501 SVIs. As mentioned in Biljecki and Ito (2021) and Yan et al. (2020), crowdsourced data, while highly beneficial due to its broad accessibility, often suffers from inconsistencies in quality and uniformity. To ensure data quality, we employed the methods described in Hou and Biljecki (2022) and Hou et al. (2024) to filter out SVIs that were blurry or had undesirable orientations (e.g., facing directly forward or to the side). Consequently, we retained 333,783 images for analysis.

Subsequently, we aggregated the SVIs within each MSOA and used the

mean values of the segmented urban objects as the input values for each neighbourhood for the constructed graphs (see Sections 3.2 and 3.3). However, it is important to note that not all MSOAs contain SVIs. Therefore, in this study, we excluded those MSOAs that lacked SVIs. As a result, we included 807 MSOAs out of a total of 983 MSOAs (including missing parts excluded in Climate Just data) for the analyses, and the number of SVIs per MSOA varies from 3 to 435.

#### *4.3. Spatial Data Collection and Preprocessing*

Due to the multifaceted nature of urban climate-related risks, which encompass a variety of factors, including socio-economic characteristics, land use patterns, and environmental features, our study collects an extensive range of spatial data, as shown in Figure 1. Our aim is to develop a comprehensive GeoAI model that incorporates these diverse urban aspects to effectively address the complex issue of urban climate justice. Below, we provide an introduction to the data used in this study in a detailed point-by-point manner.

- **Urban Road Network:** Urban road networks significantly influence urban climate justice by affecting environmental, social, and economic aspects of cities (Arsenio et al., 2016), contributing to urban heat island (Chapman et al., 2013), impacting urban resilience in risks of inland flooding (Singh et al., 2018), and resulting in social inequity (Behbahani et al., 2019). In our study, we collected open road network data from Ordnance Survey (2021). As primary traffic roads in the city often lead to a high impact on mobility and connectivity (Ceder, 2021)

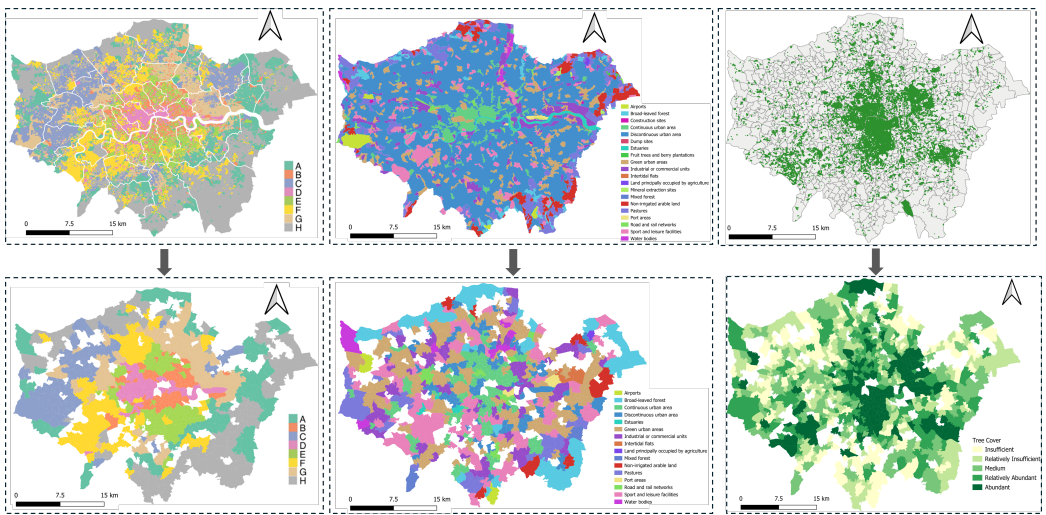


Figure 4: Data processing for LOAC, Land Cover and Tree Coverage in London. Map source licenses are the same as previous figures. For LOAC clusters, A - Intermediate Lifestyle; B - High Density and High Rise Flats; C - Settled Asians; D - Urban Elites; E - City Vibe; F - London Life-Cycle; G - Multi-Ethnic Suburbs; H - Aging City Fringe, as defined in Singleton and Longley (2015).

and result in a higher influence on urban heat and water management (Pregnolato et al., 2017), we focused on roads that carry major traffic (i.e., A and B roads in the UK road type classification<sup>3</sup>) in London for the studies.

- Urban Waterways: Urban waterways play a vital role in urban climate justice by influencing environmental health, social equity, and economic opportunities (Reckien et al., 2018). They help mitigate flood risks and manage stormwater, reducing the impact of flooding on low-income and vulnerable communities (Hashemi et al., 2024; Yereseme et al., 2022). Meanwhile, urban waterways support green spaces and vegetation, contributing to urban cooling and improving air quality by reducing the urban heat island effect (Wang et al., 2019). In our study, we collected waterway data in line format from OpenStreetMap for London, covering both natural and artificial waterways within the city, aligning with our objective to analyse the multifaceted roles of urban waterways in promoting climate justice.
- London Output Area Classification: The London Output Area Classification (LOAC) is a geodemographic tool that categorises small geographic areas based on various socio-economic and demographic characteristics (Singleton and Longley, 2015). It provides detailed insights into the diversity of London's population, helping to identify distinct

---

<sup>3</sup><https://www.gov.uk/government/publications/guidance-on-road-classification-and-the-primary-route-network/guidance-on-road-classification-and-the-primary-route-network>

groups and communities across the city. In this research, we used the LOAC provided by Singleton and Longley (2015) and calculated based on the 2011 UK census to explore if neighbourhoods that share similar geodemographics would have similar resilience when facing climate-related risks. However, LOAC was generated at output areas (OAs), which is a set of smaller-scale geographic units compared with MSOAs. Hence, to ensure the consistency of the spatial scales for each MSOA, we first aggregated the counts of LOAC categories in each MSOA and then chose the most frequent category as the socio-economic descriptor for the MSOA. For example, if the majority of OAs within an MSOA are *Ageing City Fringe* (a category in LOAC), the socio-economic descriptor for such an MSOA is *Ageing City Fringe* in the prepared dataset. If an MSOA has two LOAC categories with the same counts, we randomly picked up one as the socio-economic descriptor for this MSOA. The output map is shown in the left part of Figure 4.

- Land Cover: Land cover describes the physical characteristics of the land surface, including natural features like forests, grasslands, water bodies, and man-made structures like buildings and roads. Understanding land cover is essential for effective urban planning and sustainable development (Hassan and Nazem, 2016). We collected the land cover data from Cole et al. (2015) and proceeded to identify and extract the portions of land cover that fall within each MSOA boundary and chose the predominating types as the land cover type for the MSOA. The output map is shown in the middle part of Figure 4.

- Tree Cover: While land cover data provides a broad overview of the physical characteristics of the land surface, including natural and man-made features, an additional layer of tree cover data is necessary. Land cover data often classifies broad categories such as “forest” or “green space”, but tree cover data offers detailed information about the density and distribution of trees, which is essential for studying urban micro-climates (Kim et al., 2024; Georgi and Zafiriadis, 2006). We obtained tree distribution data for London from OpenStreetMap, aggregated the number of trees within each MSOA, and classified the tree coverage into five categories: *Abundant*, *Relatively Abundant*, *Medium*, *Relatively Insufficient*, and *Insufficient*. The output map is shown in the right part of Figure 4.

#### 4.4. Exploratory Analysis

After data had been collected and processed, we began our research by conducting preliminary exploratory data analysis on how the overall sensitivity index for both flood and heat risks, alongside the socio-spatial vulnerability indices for flooding and heat, correlated with other urban data (LC, LOAC and tree cover) collected. In this analysis, we utilised Cramér’s V correlation analysis (Cramér, 1999) to measure the strength of association between the categorical variables. Cramér’s V, derived from the Chi-square statistic, standardises the association on a scale from 0 (no association) to 1 (perfect association), rendering it especially useful for examining relationships in contingency tables with categorical data. The results of this analysis are summarised in Figure 5.

As evident from the results, the LOAC variable is most strongly correlated

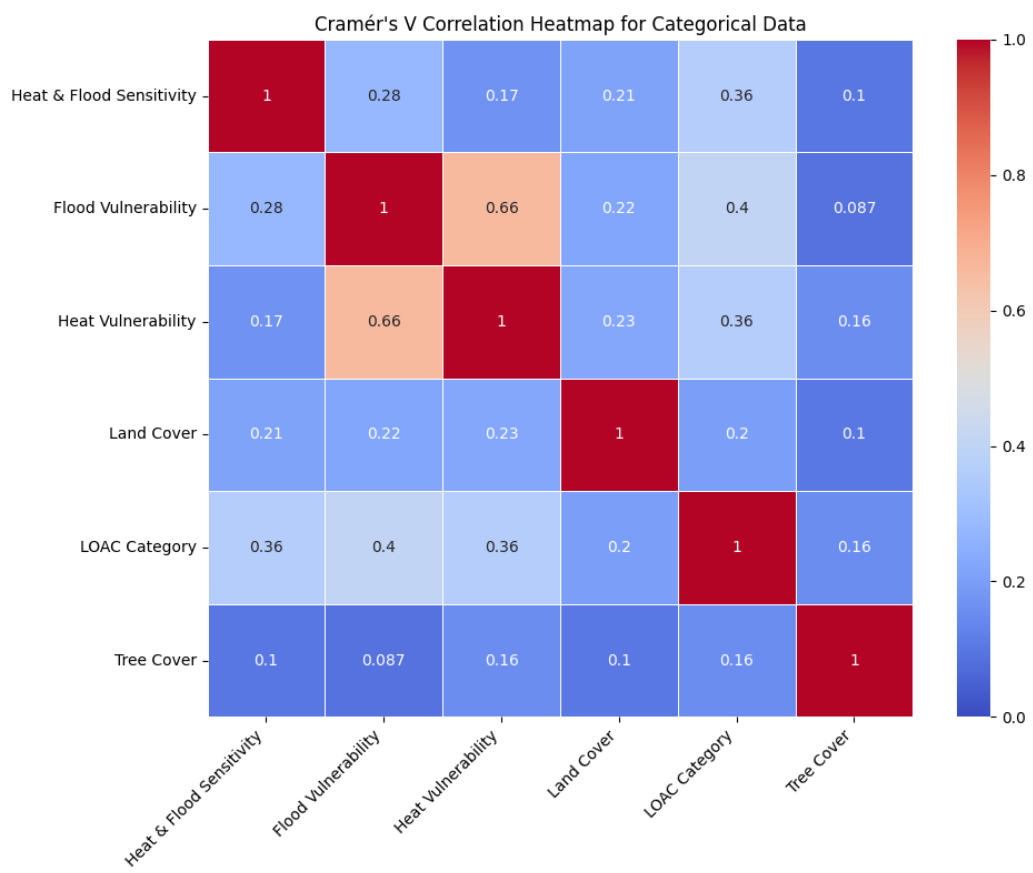


Figure 5: Cramér's V correlation analysis for the spatial data collected.

with urban sensitivity and vulnerabilities, which suggests that socio-economic factors play a key role in shaping our understanding of urban climate justice, and such a finding is later echoed in the study presented in Section 5.2. Additionally, the socio-spatial vulnerabilities to heat and flood demonstrate a strong correlation with each other, indicating that areas at high risk of flooding are also likely to experience elevated heat stress. Given their shared correlations with both LC and LOAC, this suggests that areas with similar land use and socio-economic status tend to face comparable urban risks, reinforcing conclusions drawn from previous urban environmental justice studies (Jennings et al., 2012; Reckien et al., 2018) and underscoring the rationale for why we incorporated those neighbourhood-level spatial profiles into the proposed MHGNN.

## 5. Results

The findings from the proposed study consist of two distinct sections. The first section concentrates on the performance evaluation of the MHGNN model, which targets the overall urban sensitivity to both flooding and heat stress. This involves a comparative analysis against several established baseline models, as introduced in Section 3.6. By benchmarking the MHGNN against these baselines, we aim to highlight its strengths, identify areas for improvement, and demonstrate its overall efficacy in handling urban climate justice classification tasks.

The second section delves into a series of ablation studies studying the classification performances for urban socio-spatial vulnerability to flooding and heat stress separately, as well as the overall urban sensitivity to both

Table 1: Model performance comparison against baselines.

Results	MHGNN	Random Forest	GraphSAGE	Deep Graph Infomax
Accuracy	72.23%	48.58%	28.77%	71.82%
F1 Score	70.68%	45.90%	26.12%	69.16%

flooding and heat stress. An ablation study is a method used in machine learning to assess the contribution of individual components or features of a model by systematically removing or altering them. This helps to determine the importance of each part in the model’s overall performance. In this paper, the ablation studies are designed to dissect the contributions of various genres of spatial data and the significance of different types of spatial connections. Specifically, this study investigates how pair-wise spatial connections and high-order connections among areas enhance the model’s understanding and classification of urban climate justice. By systematically removing these connections, we can pinpoint their individual and collective impacts on the model’s performance, thereby offering deeper insights into the mechanics of spatial data integration and its role in urban climate justice analysis.

### 5.1. Urban Climate Justice Classification

The outcomes of this study are detailed in Table 1, which presents a comprehensive comparison of the baseline models delineated above. As shown in the table, the MHGNN achieved the best performance among all the baselines. MHGNN’s superior performance, compared to Random Forest (RF), underscores the significance of using spatially-explicit methods in studying urban issues (Liu and Biljecki, 2022). The results clearly indicate that incorporating spatial relationships into the modelling process yields better in-

sights and more accurate predictions. Meanwhile, while DGI also delivered a reasonable performance, it highlighted the importance of simultaneously encoding both pair-wise spatial and high-order connections in the computational process for the urban climate justice classification. However, DGI falls short in terms of computational efficiency, with an inference time per sample of approximately 323  $\mu$ s compared to MHGNN’s 121  $\mu$ s. Such an efficiency gap suggests that MHGNN not only provides better accuracy but also is more suitable for applications requiring faster processing times.

On the other hand, GraphSAGE demonstrated the poorest classification performance, indicating that the simplistic approach of integrating both pair-wise spatial and high-order connections into a single matrix fails to capture the complex spatial patterns inherent in the data. The inability to adequately represent these spatial patterns highlights the necessity of investigating and utilising more sophisticated spatial data configurations to fully leverage the richness of the spatial information.

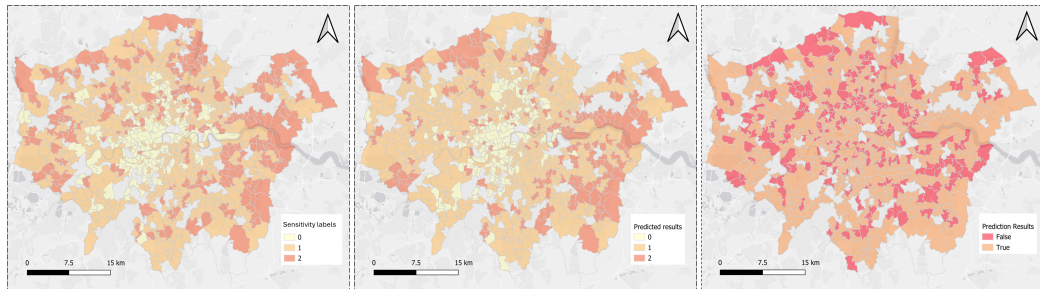


Figure 6: The left figure is the ground truth label given to the overall urban sensitivity to both flooding and heat stress; the middle figure is the predicted result; and the right figure is the spatial distribution of the errors.

A detailed examination of the classification results is provided in Figure

6. The analysis of misclassifications (i.e., errors depicted in the figure) reveals a lack of spatial autocorrelation, suggesting that MHGNN effectively captures all underlying spatial relationships present in the integrated spatial data. In other words, the MHGNN model successfully accounts for the spatial dependencies within all the data provided, thereby reducing the likelihood of geographically clustered misclassification, implying that the model has thoroughly learned the spatial patterns and relationships inherent in the data. Such a performance highlights the model’s robustness in handling complex spatial structures and suggests that MHGNN can generalise to various spatial contexts within the study area. Such a capability is crucial for urban climate justice classification, where accurately understanding and representing spatial dependencies can lead to more effective and equitable policy decisions.

As mentioned in Section 4.4, socio-economic factors play a key role in shaping our understanding of urban sensitivity and vulnerability towards heat and flooding; thus, we further investigated how the error correlates to the census statistics to examine whether the model may underperform for certain communities in the urban area. Figure 7 offers a detailed descriptive analysis of the model’s results by examining the mean and median values of census statistics associated with the errors and ground truth labels across all MSOAs. This analysis reveals that the model’s performance is less robust in areas with a representative population, suggesting potential challenges in accurately capturing the complexities of these diverse regions. Interestingly, the analysis reveals that the number of errors does not correlate with the number of SVIs in the MSOAs. Such a conclusion is supported by an

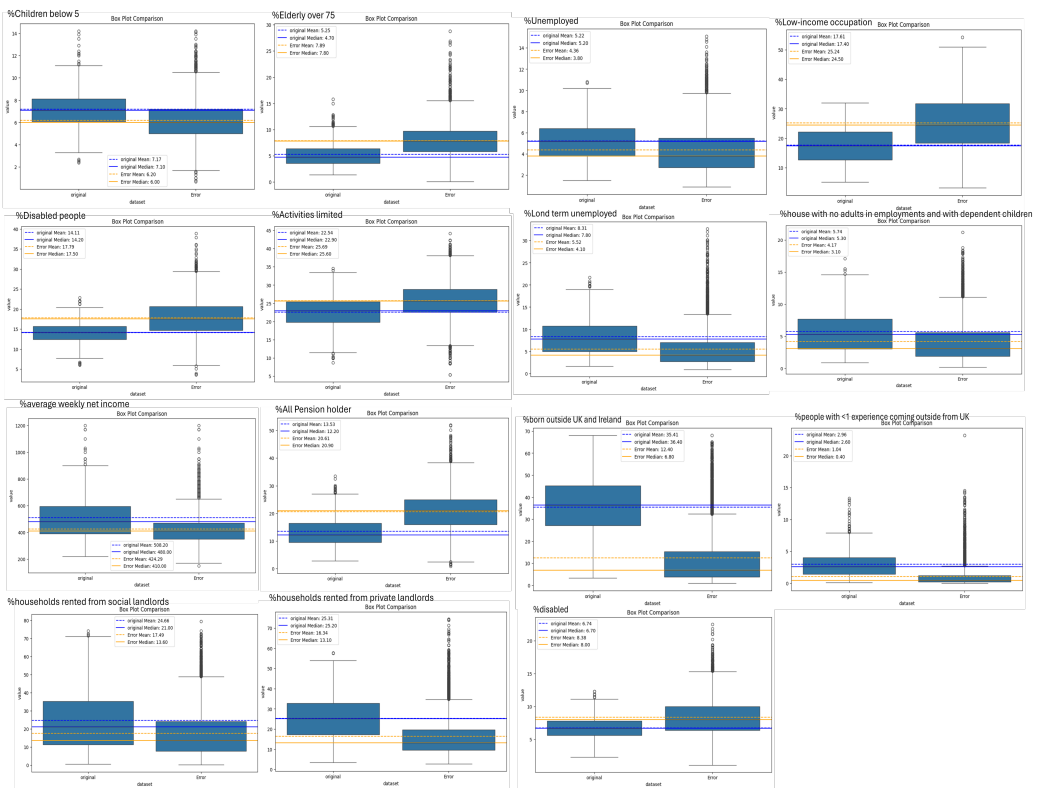


Figure 7: Descriptive analysis of the census statistics.

ANOVA test, which yields a  $p$ -value of 0.901, indicating no statistically significant relationship between the number of errors and the number of SVIs. Additionally, the Eta-Squared ( $\eta^2$ ) value of 0.015 suggests a negligible effect size, further confirming the lack of correlation. The absence of such a correlation implies that the quantity of visual data does not inherently impact the model's accuracy. However, other factors, such as the intrinsic variability within the population, might play a more significant role in influencing model performance.

### 5.2. Ablation Study

Following the assessment of the MHGNN, we implemented a series of model configurations, conducting ablation studies to identify which spatial configurations contribute to the classification performance:

- GCN-only: omits the hypergraph part of this study completely, leaving only the pair-wise spatial multigraph as the input fed into the GCN part of the MHGNN model. This examines the extent to which the high-order spatial relationships, as undermined in the Third Law of Geography (Zhu and Turner, 2022), impact the predictive performance.
- HGCN-only: omits the pair-wise spatial multigraph part of this study completely, leaving only the hypergraph as the input fed into the HGCN part of the MHGNN model. This investigates how the neighbourhood-level connections among areas, as underlined in the First Law of Geography (Tobler, 1970), impact the model performance.
- MHGNN-Roads\_Omit: omits the spatial graph constructed based on the road network in the multigraph. Road connectivity is often a cru-

cial factor in assessing socio-spatial risks related to natural hazards (Dalziell and Nicholson, 2001; Karlsson et al., 2017). By omitting this component, we can evaluate the specific contribution of the road network to the model’s predictive performance.

- MHGNN-Waterway\_Omit: omits the spatial graph constructed based on the Waterway network in the multigraph. Urban waterways are vital in assessing socio-spatial risks, as they help mitigate urban heat islands through cooling effects while also posing flood risks during heavy rainfall (Depietri et al., 2012). Their influence on the distribution of these risks, especially in vulnerable communities, is significant (Smarandon et al., 2018). By omitting the waterway component from the urban multigraph network, we aim to assess its impact on the model’s understanding of the urban environment.
- MHGNN-SpatialWeights\_Omit: omits the spatial graph constructed based on the queen contiguity spatial weights in the multigraph. Queen contiguity, which captures direct spatial relationships between neighbouring areas, is often critical in understanding spatial dependencies and clustering in geographic data (Getis and Aldstadt, 2004). By removing this component, we can isolate and assess the specific impact of these local spatial relationships on the model’s ability to capture urban spatial dynamics and predict outcomes.
- MHGNN-LOAC\_Omit: omits the high-order graph constructed based on the LOAC in the hypergraph. Socio-economic disparities across urban areas often shape climate justice (Fisher, 2015). By omitting this

component, we assess how these local neighbourhoods' socio-economic differences influence the model's performance in capturing urban dynamics and risks.

- MHGNN-LC\_Omit: omits the high-order graph constructed based on the land cover in the hypergraph. Land cover, which represents the physical characteristics of urban surfaces, is key in influencing urban environmental processes such as heat retention, water runoff, and biodiversity (Borras and Franco, 2020). By excluding this component, we aim to assess how the absence of land cover information affects the model's ability to capture critical environmental factors and predict spatial risks in urban areas.
- MHGNN-Tree\_Omit: omits the high-order graph constructed based on the tree coverage level in the hypergraph. Tree coverage impacts urban microclimates by providing shade, reducing heat stress, and mitigating flood risks through improved water absorption (Schwarz et al., 2015). By excluding this component, we evaluate how the absence of tree-related spatial information affects the model's capacity to account for environmental resilience and predict risks in urban settings.

The results are summarised in Table 2 and reveal several interesting insights, underscoring the importance of different spatial configurations in understanding urban environments. Firstly, the inclusion of high-order connections in spatial modelling provides a comprehensive understanding of urban settings, echoing findings from previous studies by Wang and Zhu (2024), which highlights the value of considering complex spatial relationships be-

Table 2: Albation Studies on the spatial graphs.

Features	GCN-only	HGCN-only	Roads_Omit	Waterway_Omit	SpatialWights_Omit	LOAC_Omit	LC_Omit	Tree_Omit
Spatial Weights	✓		✓	✓		✓	✓	✓
Roads	✓			✓	✓	✓	✓	✓
Waterway	✓		✓		✓	✓	✓	✓
LOAC		✓	✓	✓	✓		✓	✓
LC		✓	✓	✓	✓	✓		✓
Tree		✓	✓	✓	✓	✓	✓	
Accuracy (Flood and Heat)	61.66%	65.19%	67.27%	66.91%	66.02%	63.23%	66.67%	65.92%
F1 Score (Flood and Heat)	58.11%	61.51%	66.75%	64.79%	63.22%	61.37%	64.75%	62.16%
Accuracy (Flood)	67.32%	63.88%	64.41%	61.15%	63.73%	61.23%	64.93%	67.10%
F1 Score (Flood)	64.23%	60.87%	61.55%	58.76%	59.01%	58.55%	61.73%	66.82%
Accuracy (Heat)	61.21%	65.49%	64.77%	62.71%	63.26%	60.11%	63.55%	63.17%
F1 Score (Heat)	59.88%	63.75%	62.17%	60.78%	60.82%	57.95%	62.34%	60.25%

yond simple pair-wise connections. The results also indicate a differential impact of spatial configurations on various types of urban vulnerability classifications. Specifically, pair-wise spatial connections contribute more significantly to the classification of urban socio-spatial flooding vulnerability. In contrast, high-order connections are more influential in the classification of heat-related vulnerability. Such a distinction suggests that different types of urban vulnerabilities are characterised by different spatial interaction patterns, necessitating tailored modelling approaches for each. Additionally, LOAC, a geodemographic classification of urban areas, emerges evidently as a particularly strong influence on the classifications among all the high-order connections, which underscores the critical importance of incorporating socio-economic indicators in urban analytics (Wang et al., 2024; Liu and Biljecki, 2022).

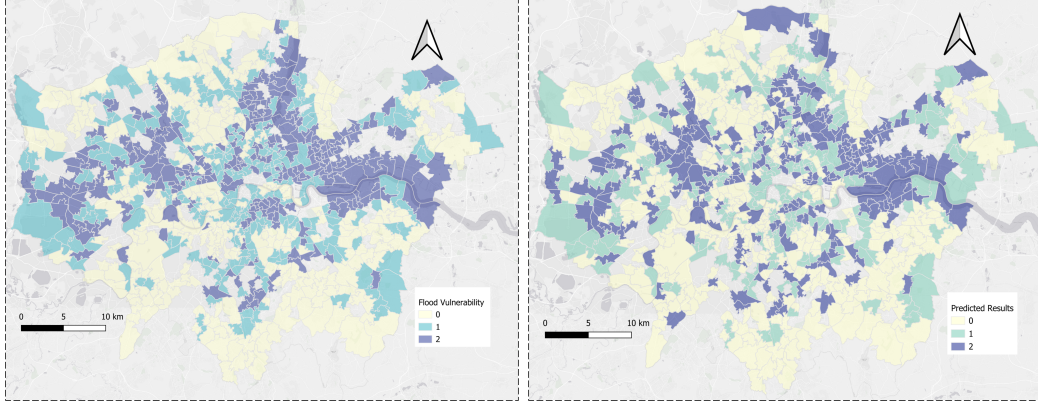


Figure 8: Urban socio-spatial flooding vulnerability comparison. Left figure: labels in Climate Just data; right figure: predicted results using MHGNN.

## 6. Scenario Understanding: Classifying Recent Urban Flooding Risks in London

The previous sections highlighted the effectiveness of our proposed MHGNN model in classifying urban climate-related risks using spatial configurations and SVIs as inputs. The initial studies were based on the London Climate Just dataset, utilising the 2011 UK Census data. To obtain a more current understanding of urban climate justice and to further validate our model’s applicability, this section presents a use case scenario employing the latest data to classify urban risks.

Recognising flooding as the main environmental risk to people living in London (Bates et al., 2023), our case study focused on the urban socio-spatial flooding vulnerability in London using the pre-trained MHGNN. We further collected SVIs from Mappillary between the 23<sup>rd</sup> of September 2022 and the 1<sup>st</sup> of June 2024 and combined the dataset with previously collected data introduced in Section 4.2. Meanwhile, for LOAC introduced in Section 4.3, we

replaced it using the most recent LOAC produced by Singleton and Longley (2024) to incorporate the most recent socio-economic urban indicators in the model. All other spatial configurations remained the same as before. Figure 8 shows the new classification result. Such results suggest an increasing condition on how London improved the urban environment in handling urban flooding risks. Specifically, approximately 20% of the areas have shifted from medium vulnerability to low vulnerability, and 12% of the areas have moved from high vulnerability to medium vulnerability, indicating successful efforts delivered by local authorities to address flooding risks in the past decade (Bang and Burton, 2021).

## 7. Discussion and Conclusion

This paper presents a GeoAI approach, the Multi-Hyper Graph Neural Network (MHGNN) that combines a multigraph and a hypergraph to model complex spatial patterns in classifying urban climate justice in urban areas. The multigraph component of the MHGNN focuses on pair-wise spatial connections among geographic areas, and it incorporates these spatial relationships into a sophisticated graph modelling process. By considering the proximities of different areas and the connections in between (i.e., road networks, waterways and queen contiguity spatial weights), the multigraph component accurately reflects the First Law of Geography, which posits that “everything is related to everything else, but near things are more related than distant things” (Tobler, 1970), ensuring that the model accounts for the influence of geographical proximity on urban climate justice outcomes. Meanwhile, the hypergraph component of the MHGNN addresses the Third

Law of Geography, which suggests that “the more similar the geographic settings of two places, the more similar the phenomena that occur in those places” (Zhu and Turner, 2022). By incorporating hyperedges that connect multiple geographic areas based on their similarity, the hypergraph effectively captures the nuanced and multi-faceted relationships between areas with comparable geographic settings. This enables the model to account for the influence of shared geographic characteristics on urban climate justice beyond mere spatial proximity. By leveraging the strengths of both multigraph and hypergraph structures, the MHGNN offers a comprehensive understanding of the spatial dynamics of urban climate justice, positioning it as a valuable tool for researchers and policymakers working in this field.

Echoing the findings of Wang and Zhu (2024), our research underscores the effectiveness of utilising hyperedges to capture high-order connections among geographic areas. Such an approach allows areas that are geographically distant to be connected if they share similar conceptual level categories, such as LOAC. Our results reveal the particular utility of socio-economic indicators in high-order spatial modelling, demonstrating that socio-economic-driven classifications of urban areas are crucial for understanding the urban vulnerabilities to climate-related risks at the neighbourhood level. However, our research also highlights a significant challenge. While the MHGNN proved capable of delivering reasonable results in identifying urban socio-spatial vulnerabilities, its performance fell short in urban areas with under-represented groups. This finding indicates the need for additional tailored modelling to accurately represent the diverse populations in metropolitan cities like London. Addressing this shortcoming is essential to mitigate po-

tential biases inherent in algorithm-driven analyses (Van Migerode et al., 2024; Ingold and Soper, 2016; Shelton et al., 2014).

Recognising crowdsourced street view imagery (SVIs) as a valuable source to study the urban environment (Hou et al., 2024; Zhang et al., 2024a; Biljecki et al., 2023; Juhasz and Hochmair, 2016; Ding et al., 2021), our study demonstrates that SVIs offer a cost-effective and timely alternative to traditional census statistics for analysing socio-spatial urban challenges, including climate justice. Unlike census data, which is typically collected at periodic intervals and may quickly become outdated, SVIs are updated much more frequently. Such a continuous influx of fresh visual data allows researchers to monitor and assess urban environments in near real-time, providing insights into rapidly changing urban dynamics. Furthermore, the use of SVIs democratises data collection and analysis, as these images are often crowdsourced from a diverse array of contributors. Although the model presents less robust for underrepresented populations, from the data perspective, the non-statistically significant relationship between the errors of the classification and the number of SVIs showcases the representativeness of the data, ensuring that the perspectives of different community members are reflected in the analysis.

Several directions will be pursued in our future studies to enhance the understanding and modelling of urban climate justice. First, we aim to improve the spatial modelling capabilities of the MHGNN to better predict outcomes for underrepresented populations. One possible solution is to incorporate the UK Multiple Deprivation Indices (Morse, 2024) into the high-order spatial modelling framework, which helps to fill in the socio-economic gaps that

the LOAC may inherently miss, thereby providing a more comprehensive socio-economic profile of urban areas. By doing so, we aim to ensure that the predictive power of the MHGNN is robust across diverse demographic groups, ultimately leading to more equitable urban climate justice outcomes. Second, we plan to expand our data sources beyond crowdsourced SVIs. Integrating satellite imagery and 3D city models will be a crucial direction to explore. Satellite imagery can provide macro-level insights into urban environmental conditions, such as heat islands and vegetation cover, while 3D models can offer detailed representations of urban morphology and infrastructure. This multi-dimensional data infusion will enable a richer and more precise analysis of urban spatial patterns and their impact on climate justice. Third, our future research will also shed light on the participatory urban planning process in addressing urban climate justice. By formalising a specialised team from the local residents for SVIs and urban infrastructure data collection, the multi-dimensional data integration will lead to more inclusive urban development strategies that reflect the diverse needs and preferences of urban residents, hence potentially enhancing the model's predictive powers. Last but not least, we plan to extend the application of the MHGNN model to real-world scenarios by studying and classifying urban climate justice across various urban contexts. This will involve applying MHGNN to cities with distinct urban characteristics, allowing us to explore how the model can be tailored to address the specific challenges posed by different spatial configurations, environmental risks, and socio-economic conditions. By adapting the framework to diverse settings, we aim to demonstrate its versatility and practical relevance in addressing urban climate justice issues

globally, thus supporting informed decision-making in urban planning and climate resilience strategies across different city environments.

## Acknowledgements

We thank the members of the NUS Urban Analytics Lab and Dr Yuhao Kang from the University of Texas at Austin for the discussions. We also thank Ms Yujun Hou for the initial SVI data collection. The research was conducted at the Future Cities Lab Global at the Singapore-ETH Centre, which was established collaboratively between ETH Zurich and the National Research Foundation Singapore. This research is supported by the National Research Foundation Singapore (NRF) under its Campus for Research Excellence and Technological Enterprise (CREATE) programme. This research is also supported by the Humanities Social Sciences Seed Fund at the National University of Singapore (A-8001957-00-00). This research is also supported by the project Multi-scale Digital Twins for the Urban Environment: From Heartbeats to Cities, which is supported by the Singapore Ministry of Education Academic Research Fund Tier 1. This research is also part of the project Large-scale 3D Geospatial Data for Urban Analytics, which is supported by the National University of Singapore under the Start-Up Grant R-295-000-171-133.

## References

- Ameer, S., Shah, M.A., 2018. Exploiting big data analytics for smart urban planning, in: 2018 IEEE 88th Vehicular Technology Conference (VTC-Fall), IEEE. pp. 1–5.

- Amorim-Maia, A.T., Anguelovski, I., Chu, E., Connolly, J., 2022. Intersectoral climate justice: A conceptual pathway for bridging adaptation planning, transformative action, and social equity. *Urban climate* 41, 101053.
- Apte, J.S., Messier, K.P., Gani, S., Brauer, M., Kirchstetter, T.W., Lundin, M.M., Marshall, J.D., Portier, C.J., Vermeulen, R.C., Hamburg, S.P., 2017. High-resolution air pollution mapping with google street view cars: exploiting big data. *Environmental science & technology* 51, 6999–7008.
- Aroca-Jiménez, E., Bodoque, J.M., García, J.A., 2020. How to construct and validate an integrated socio-economic vulnerability index: Implementation at regional scale in urban areas prone to flash flooding. *Science of the Total Environment* 746, 140905.
- Arsenio, E., Martens, K., Di Ciommo, F., 2016. Sustainable urban mobility plans: Bridging climate change and equity targets? *Research in Transportation Economics* 55, 30–39.
- Bai, S., Zhang, F., Torr, P.H., 2021. Hypergraph convolution and hypergraph attention. *Pattern Recognition* 110, 107637.
- Bang, H.N., Burton, N.C., 2021. Contemporary flood risk perceptions in england: Implications for flood risk management foresight. *Climate Risk Management* 32, 100317.
- Bates, P.D., Savage, J., Wing, O., Quinn, N., Sampson, C., Neal, J., Smith, A., 2023. A climate-conditioned catastrophe risk model for uk flooding. *Natural Hazards and Earth System Sciences* 23, 891–908.

Behbahani, H., Nazari, S., Partovifar, H., Kang, M.J., 2019. Designing a road network using john rawls's social justice approach. *Journal of Urban Planning and Development* 145, 05019002.

Ben-Joseph, E., Lee, J.S., Cromley, E.K., Laden, F., Troped, P.J., 2013. Virtual and actual: relative accuracy of on-site and web-based instruments in auditing the environment for physical activity. *Health & place* 19, 138–150.

Benz, S.A., Burney, J.A., 2021. Widespread race and class disparities in surface urban heat extremes across the united states. *Earth's Future* 9, e2021EF002016.

Biljecki, F., Ito, K., 2021. Street view imagery in urban analytics and gis: A review. *Landscape and Urban Planning* 215, 104217.

Biljecki, F., Zhao, T., Liang, X., Hou, Y., 2023. Sensitivity of measuring the urban form and greenery using street-level imagery: A comparative study of approaches and visual perspectives. *International Journal of Applied Earth Observation and Geoinformation* 122, 103385. doi:10.1016/j.jag.2023.103385.

Boller, D., Moy de Vitry, M., D. Wegner, J., Leitão, J.P., 2019. Automated localization of urban drainage infrastructure from public-access street-level images. *Urban Water Journal* 16, 480–493.

Borras, S.M., Franco, J.C., 2020. The challenge of locating land-based climate change mitigation and adaptation politics within a social justice per-

- spective: towards an idea of agrarian climate justice, in: Converging Social Justice Issues and Movements. Routledge, pp. 82–99.
- Broto, V.C., Bulkeley, H., 2013. A survey of urban climate change experiments in 100 cities. *Global environmental change* 23, 92–102.
- Bulkeley, H., Carmin, J., Broto, V.C., Edwards, G.A., Fuller, S., 2013. Climate justice and global cities: Mapping the emerging discourses. *Global environmental change* 23, 914–925.
- Bulkeley, H., Edwards, G.A., Fuller, S., 2014. Contesting climate justice in the city: Examining politics and practice in urban climate change experiments. *Global Environmental Change* 25, 31–40.
- Cao, C., Lam, N.S.N., 2023. Understanding the scale and resolution effects in remote sensing and gis, in: Scale in remote sensing and GIS. Routledge, pp. 57–72.
- Ceder, A., 2021. Urban mobility and public transport: future perspectives and review. *International Journal of Urban Sciences* 25, 455–479.
- Chang, L.F., Huang, S.L., 2015. Assessing urban flooding vulnerability with an emergy approach. *Landscape and Urban Planning* 143, 11–24.
- Chapman, L., Azevedo, J.A., Prieto-Lopez, T., 2013. Urban heat & critical infrastructure networks: A viewpoint. *Urban Climate* 3, 7–12.
- Chen, L.C., Papandreou, G., Kokkinos, I., Murphy, K., Yuille, A.L., 2017. Deeplab: Semantic image segmentation with deep convolutional nets,

- atrous convolution, and fully connected crfs. *IEEE transactions on pattern analysis and machine intelligence* 40, 834–848.
- Cheng, Z., Nesbitt, L., Girling, C., Sheppard, S., Konijnendijk, C., Nitoslawski, S., 2024. Urban density and the urban forest: How well are cities balancing them in the context of climate change? *Cities* 149, 104962.
- Cole, B., King, S., Ongutu, B., Plamer, D., Smith, G., Balzter, H., 2015. Corine land cover 2012 for the uk, jersey and guernsey .
- Coleman, D., 2013. The twilight of the census. *PoPulation and developPment review* 38, 334–351.
- Cordts, M., Omran, M., Ramos, S., Rehfeld, T., Enzweiler, M., Benenson, R., Franke, U., Roth, S., Schiele, B., 2016. The cityscapes dataset for semantic urban scene understanding, in: *Proceedings of the IEEE conference on computer vision and pattern recognition*, pp. 3213–3223.
- Cramér, H., 1999. Mathematical methods of statistics. volume 26. Princeton university press.
- Dalziell, E., Nicholson, A., 2001. Risk and impact of natural hazards on a road network. *Journal of transportation engineering* 127, 159–166.
- De Sabbata, S., Ballatore, A., Liu, P., Tate, N., 2023a. Learning urban form through unsupervised graph-convolutional neural networks, in: *The 2nd International Workshop on Geospatial Knowledge Graphs and GeoAI: Methods, Models, and Resources*.

- De Sabbata, S., Ballatore, A., Miller, H.J., Sieber, R., Tyukin, I., Yeboah, G., 2023b. Geoai in urban analytics.
- De Sabbata, S., Liu, P., 2023. A graph neural network framework for spatial geodemographic classification. International Journal of Geographical Information Science 37, 2464–2486.
- Depietri, Y., Renaud, F.G., Kallis, G., 2012. Heat waves and floods in urban areas: a policy-oriented review of ecosystem services. Sustainability science 7, 95–107.
- Dharmarathne, G., Waduge, A., Bogahawaththa, M., Rathnayake, U., Meddage, D., 2024. Adapting cities to the surge: A comprehensive review of climate-induced urban flooding. Results in Engineering , 102123.
- Ding, X., Fan, H., Gong, J., 2021. Towards generating network of bikeways from mapillary data. Computers, Environment and Urban Systems 88, 101632. doi:10.1016/j.compenvurbsys.2021.101632.
- Ebi, K.L., Capon, A., Berry, P., Broderick, C., de Dear, R., Harenith, G., Honda, Y., Kovats, R.S., Ma, W., Malik, A., et al., 2021. Hot weather and heat extremes: health risks. The lancet 398, 698–708.
- Fey, M., Lenssen, J.E., 2019. Fast graph representation learning with PyTorch Geometric, in: ICLR Workshop on Representation Learning on Graphs and Manifolds.
- Fisher, S., 2015. The emerging geographies of climate justice. The Geographical Journal 181, 73–82.

- Georgi, N.J., Zafiriadis, K., 2006. The impact of park trees on microclimate in urban areas. *Urban Ecosystems* 9, 195–209.
- Getis, A., Aldstadt, J., 2004. Constructing the spatial weights matrix using a local statistic. *Geographical analysis* 36, 90–104.
- Hamilton, W., Ying, Z., Leskovec, J., 2017. Inductive representation learning on large graphs. *Advances in neural information processing systems* 30.
- Hashemi, F., Mills, G., Poerschke, U., Iulo, L.D., Pavlak, G., Kalisperis, L., 2024. A novel parametric workflow for simulating urban heat island effects on residential building energy use: Coupling local climate zones with the urban weather generator a case study of seven us cities. *Sustainable Cities and Society* , 105568.
- Hassan, M.M., Nazem, M.N.I., 2016. Examination of land use/land cover changes, urban growth dynamics, and environmental sustainability in chittagong city, bangladesh. *Environment, development and sustainability* 18, 697–716.
- Hofflinger, A., Somos-Valenzuela, M.A., Vallejos-Romero, A., 2019. Response time to flood events using a social vulnerability index (retsvi). *Natural hazards and earth system sciences* 19, 251–267.
- Hou, Y., Biljecki, F., 2022. A comprehensive framework for evaluating the quality of street view imagery. *International Journal of Applied Earth Observation and Geoinformation* 115, 103094.
- Hou, Y., Quintana, M., Khomiakov, M., Yap, W., Ouyang, J., Ito, K., Wang, Z., Zhao, T., Biljecki, F., 2024. Global streetscapes—a comprehensive

dataset of 10 million street-level images across 688 cities for urban science and analytics. ISPRS Journal of Photogrammetry and Remote Sensing 215, 216–238.

Huang, X., Wang, S., Yang, D., Hu, T., Chen, M., Zhang, M., Zhang, G., Biljecki, F., Lu, T., Zou, L., et al., 2024. Crowdsourcing geospatial data for earth and human observations: A review. Journal of Remote Sensing 4, 0105.

Ingold, D., Soper, S., 2016. Amazon doesn't consider the race of its customers. should it? bloomberg, april 21, 2016.

Ito, K., Kang, Y., Zhang, Y., Zhang, F., Biljecki, F., 2024. Understanding urban perception with visual data: A systematic review. Cities 152, 105169.

Jenks, G.F., 1975. The evaluation and prediction of visual clustering in maps symbolized with proportional circles. DAVIS, J.; MACCULLAUGH, M. Display and Analysis of Spatial Data. New York: Wiley , 311–327.

Jennings, V., Johnson Gaither, C., Gragg, R.S., 2012. Promoting environmental justice through urban green space access: A synopsis. Environmental justice 5, 1–7.

Juhasz, L., Hochmair, H.H., 2016. User contribution patterns and completeness evaluation of mapillary, a crowdsourced street level photo service. Transactions in GIS 20, 925–947. doi:10.1111/tgis.12190.

Karanja, J., Kiage, L., 2021. Perspectives on spatial representation of urban heat vulnerability. Science of The Total Environment 774, 145634.

- Karlsson, C.S., Kalantari, Z., Mörtsberg, U., Olofsson, B., Lyon, S.W., 2017. Natural hazard susceptibility assessment for road planning using spatial multi-criteria analysis. *Environmental management* 60, 823–851.
- Keat, W.J., Kendon, E.J., Bohnenstengel, S.I., 2021. Climate change over uk cities: the urban influence on extreme temperatures in the uk climate projections. *Climate dynamics* 57, 3583–3597.
- Kim, E.S., Yun, S.H., Park, C.Y., Heo, H.K., Lee, D.K., 2022. Estimation of mean radiant temperature in urban canyons using google street view: A case study on seoul. *Remote Sensing* 14, 260.
- Kim, J., Ewing, R., Rigolon, A., 2024. Does green infrastructure affect housing prices via extreme heat and air pollution mitigation? a focus on green and climate gentrification in los angeles county, 2000-2021. *Sustainable Cities and Society* 102, 105225.
- Kim, S.W., Brown, R.D., 2021. Urban heat island (uhi) variations within a city boundary: A systematic literature review. *Renewable and Sustainable Energy Reviews* 148, 111256.
- Kingma, D.P., Ba, J., 2014. Adam: A method for stochastic optimization. arXiv preprint arXiv:1412.6980 .
- Kipf, T.N., Welling, M., 2016. Semi-supervised classification with graph convolutional networks. arXiv preprint arXiv:1609.02907 .
- Koks, E.E., Jongman, B., Husby, T.G., Botzen, W.J., 2015. Combining hazard, exposure and social vulnerability to provide lessons for flood risk management. *Environmental science & policy* 47, 42–52.

- Lamond, J.E., Proverbs, D., Hammond, F., 2009. Accessibility of flood risk insurance in the uk: confusion, competition and complacency. *Journal of Risk Research* 12, 825–841.
- Lankao, P.R., Qin, H., 2011. Conceptualizing urban vulnerability to global climate and environmental change. *Current opinion in environmental sustainability* 3, 142–149.
- Latham, Z., Barrett-Lennard, G., Opdyke, A., 2024. Archetypes of local governance for flood risk reduction decision-making under uncertain climate change futures. *Sustainable Cities and Society* 112, 105632. URL: <https://www.sciencedirect.com/science/article/pii/S2210670724004578>, doi:<https://doi.org/10.1016/j.scs.2024.105632>.
- Lavallin, A., Downs, J.A., 2021. Machine learning in geography—past, present, and future. *Geography Compass* 15, e12563.
- Li, X., Ratti, C., 2019. Mapping the spatio-temporal distribution of solar radiation within street canyons of boston using google street view panoramas and building height model. *Landscape and urban planning* 191, 103387.
- Li, X., Zhang, C., Li, W., 2015a. Does the visibility of greenery increase perceived safety in urban areas? evidence from the place pulse 1.0 dataset. *ISPRS International Journal of Geo-Information* 4, 1166–1183.
- Li, X., Zhang, C., Li, W., Ricard, R., Meng, Q., Zhang, W., 2015b. Assessing street-level urban greenery using google street view and a modified green view index. *Urban Forestry & Urban Greening* 14, 675–685.

Lindley, S., Kazmierczak, A., Connelly, A., Robinson, C., O'Neill, J., 2014. Climate just. URL: <https://www.climatejust.org.uk/>.

Liu, P., Biljecki, F., 2022. A review of spatially-explicit geoai applications in urban geography. International Journal of Applied Earth Observation and Geoinformation 112, 102936.

Liu, P., Zhang, Y., Biljecki, F., 2024. Explainable spatially explicit geospatial artificial intelligence in urban analytics. Environment and Planning B: Urban Analytics and City Science 51, 1104–1123.

Liu, P., Zhao, T., Luo, J., Lei, B., Frei, M., Miller, C., Biljecki, F., 2023. Towards human-centric digital twins: leveraging computer vision and graph models to predict outdoor comfort. Sustainable Cities and Society 93, 104480.

Liu, Y., Chu, L., Chen, G., Wu, Z., Chen, Z., Lai, B., Hao, Y., 2021. Paddleseg: A high-efficient development toolkit for image segmentation. [arXiv:2101.06175](https://arxiv.org/abs/2101.06175).

Lu, Y., Chen, H.M., 2024. Using google street view to reveal environmental justice: Assessing public perceived walkability in macroscale city. Landscape and Urban Planning 244, 104995.

Lu, Y., Ferranti, E.J.S., Chapman, L., Pfrang, C., 2023. Assessing urban greenery by harvesting street view data: A review. Urban Forestry & Urban Greening 83, 127917.

- Luo, J., Zhao, T., Cao, L., Biljecki, F., 2022. Semantic riverscapes: Perception and evaluation of linear landscapes from oblique imagery using computer vision. *Landscape and Urban Planning* 228, 104569.
- Ma, D., He, F., Yue, Y., Guo, R., Zhao, T., Wang, M., 2024. Graph convolutional networks for street network analysis with a case study of urban polycentricity in chinese cities. *International Journal of Geographical Information Science* 38, 931–955.
- Ma, H., Xu, Q., Zhang, Y., 2023. High or low? exploring the restorative effects of visual levels on campus spaces using machine learning and street view imagery. *Urban Forestry & Urban Greening* 88, 128087.
- Mai, G., Janowicz, K., Hu, Y., Gao, S., Yan, B., Zhu, R., Cai, L., Lao, N., 2022. A review of location encoding for geoai: methods and applications. *International Journal of Geographical Information Science* 36, 639–673.
- Mignot, E., Dewals, B., 2022. Hydraulic modelling of inland urban flooding: recent advances. *Journal of hydrology* 609, 127763.
- Morse, S., 2024. Index of multiple deprivation (imd)(uk), in: *Encyclopedia of Quality of Life and Well-Being Research*. Springer, pp. 3440–3443.
- Nair, V., Hinton, G.E., 2010. Rectified linear units improve restricted boltzmann machines, in: *Proceedings of the 27th international conference on machine learning (ICML-10)*, pp. 807–814.
- Nathvani, R., Vishwanath, D., Clark, S.N., Alli, A.S., Muller, E., Coste, H., Bennett, J.E., Nimo, J., Moses, J.B., Baah, S., et al., 2023. Beyond

here and now: Evaluating pollution estimation across space and time from street view images with deep learning. *Science of the Total Environment* 903, 166168.

Ordnance Survey, 2021. Os open roads.  
<https://www.ordnancesurvey.co.uk/products/os-open-roads#overview>. Accessed: 2024-06-14.

PaddlePaddle Authors, 2019. Paddleseg, end-to-end image segmentation kit based on paddlepaddle. <https://github.com/PaddlePaddle/PaddleSeg>.

Park, C.Y., Lee, D.K., Asawa, T., Murakami, A., Kim, H.G., Lee, M.K., Lee, H.S., 2019. Influence of urban form on the cooling effect of a small urban river. *Landscape and urban planning* 183, 26–35.

Park, C.Y., Thorne, J.H., Hashimoto, S., Lee, D.K., Takahashi, K., 2021. Differing spatial patterns of the urban heat exposure of elderly populations in two megacities identifies alternate adaptation strategies. *Science of the Total Environment* 781, 146455.

Paszke, A., Gross, S., Massa, F., Lerer, A., Bradbury, J., Chanan, G., Killeen, T., Lin, Z., Gimelshein, N., Antiga, L., et al., 2019. Pytorch: An imperative style, high-performance deep learning library. *Advances in neural information processing systems* 32.

Percival, S.E., Gaterell, M., Hutchinson, D., 2020. Effective flood risk visualisation. *Natural Hazards* 104, 375–396.

Porter, L., Rickards, L., Verlie, B., Bosomworth, K., Moloney, S., Lay, B.,

- Latham, B., Anguelovski, I., Pellow, D., 2020. Climate justice in a climate changed world. *Planning Theory & Practice* 21, 293–321.
- Pregnolato, M., Ford, A., Glenis, V., Wilkinson, S., Dawson, R., 2017. Impact of climate change on disruption to urban transport networks from pluvial flooding. *Journal of Infrastructure Systems* 23, 04017015.
- Price, A., Jones, E.C., Jefferson, F., 2015. Vertical greenery systems as a strategy in urban heat island mitigation. *Water, Air, & Soil Pollution* 226, 1–11.
- Puissant, A., Rougier, S., Stumpf, A., 2014. Object-oriented mapping of urban trees using random forest classifiers. *International Journal of Applied Earth Observation and Geoinformation* 26, 235–245.
- Qi, M., Hankey, S., 2021. Using street view imagery to predict street-level particulate air pollution. *Environmental Science & Technology* 55, 2695–2704.
- Rahmani, S., Baghbani, A., Bouguila, N., Patterson, Z., 2023. Graph neural networks for intelligent transportation systems: A survey. *IEEE Transactions on Intelligent Transportation Systems* 24, 8846–8885.
- Reckien, D., Lwasa, S., Satterthwaite, D., McEvoy, D., Creutzig, F., Montgomery, M., Schensul, D., Balk, D., Khan, I.A., Fernandez, B., et al., 2018. Equity, environmental justice, and urban climate change, in: Climate change and cities: Second assessment report of the urban climate change research network. Cambridge University Press, pp. 173–224.

- Rubinato, M., Nichols, A., Peng, Y., Zhang, J.m., Lashford, C., Cai, Y.p., Lin, P.z., Tait, S., 2019. Urban and river flooding: Comparison of flood risk management approaches in the uk and china and an assessment of future knowledge needs. *Water science and engineering* 12, 274–283.
- Rui, Q., Cheng, H., 2023. Quantifying the spatial quality of urban streets with open street view images: A case study of the main urban area of fuzhou. *Ecological Indicators* 156, 111204.
- Rundle, A.G., Bader, M.D., Richards, C.A., Neckerman, K.M., Teitler, J.O., 2011. Using google street view to audit neighborhood environments. *American journal of preventive medicine* 40, 94–100.
- Sayers, P., Horritt, M., Penning Rowsell, E., Fieth, J., 2017. Present and future flood vulnerability, risk and disadvantage a uk assessment prepared for joseph rowntree foundation, climate change and communities programme.
- Schlosberg, D., Collins, L.B., 2014. From environmental to climate justice: climate change and the discourse of environmental justice. *Wiley Interdisciplinary Reviews: Climate Change* 5, 359–374.
- Schreider, S.Y., Smith, D., Jakeman, A., 2000. Climate change impacts on urban flooding. *Climatic Change* 47, 91–115.
- Schwarz, K., Fragkias, M., Boone, C.G., Zhou, W., McHale, M., Grove, J.M., O’Neil-Dunne, J., McFadden, J.P., Buckley, G.L., Childers, D., et al., 2015. Trees grow on money: urban tree canopy cover and environmental justice. *PloS one* 10, e0122051.

- Sebestyen, V., Dorgo, G., Ipkovich, A., Abonyi, J., 2023. Identifying the links among urban climate hazards, mitigation and adaptation actions and sustainability for future resilient cities. *Urban Climate* 49, 101557. URL: <https://www.sciencedirect.com/science/article/pii/S2212095523001517>, doi:<https://doi.org/10.1016/j.uclim.2023.101557>.
- Shelton, T., Poorthuis, A., Graham, M., Zook, M., 2014. Mapping the data shadows of hurricane sandy: Uncovering the socio-spatial dimensions of ‘big data’. *Geoforum* 52, 167–179.
- Shi, L., Chu, E., Anguelovski, I., Aylett, A., Debats, J., Goh, K., Schenk, T., Seto, K.C., Dodman, D., Roberts, D., et al., 2016. Roadmap towards justice in urban climate adaptation research. *Nature Climate Change* 6, 131–137.
- Singh, P., Sinha, V.S.P., Vijhani, A., Pahuja, N., 2018. Vulnerability assessment of urban road network from urban flood. *International journal of disaster risk reduction* 28, 237–250.
- Singleton, A.D., Longley, P., 2015. The internal structure of greater london: a comparison of national and regional geodemographic models. *Geo: Geography and Environment* 2, 69–87.
- Singleton, A.D., Longley, P.A., 2024. Classifying and mapping residential structure through the london output area classification. *Environment and Planning B: Urban Analytics and City Science* 51, 1153–1164.
- Smardon, R., Moran, S., Baptiste, A.K., 2018. Revitalizing urban waterway communities: Streams of environmental justice. Routledge.

Steele, W., Mata, L., Füngfeld, H., 2015. Urban climate justice: creating sustainable pathways for humans and other species. *Current opinion in environmental sustainability* 14, 121–126.

Sultana, F., 2022. Critical climate justice. *The Geographical Journal* 188, 118–124.

Surminski, S., Westcott, M., Ward, J., Sayers, P., Bresch, D., Clare, B., 2020. Be prepared—exploring future climate-related risk for residential and commercial real-estate portfolios. *Journal of Alternative Investments* 23, 24–34.

Taylor, J., Wilkinson, P., Davies, M., Armstrong, B., Chalabi, Z., Mavrogianni, A., Symonds, P., Oikonomou, E., Bohnenstengel, S.I., 2015. Mapping the effects of urban heat island, housing, and age on excess heat-related mortality in london. *Urban Climate* 14, 517–528.

Tobler, W.R., 1970. A computer movie simulating urban growth in the detroit region. *Economic geography* 46, 234–240.

Tuholske, C., Caylor, K., Funk, C., Verdin, A., Sweeney, S., Grace, K., Peterson, P., Evans, T., 2021. Global urban population exposure to extreme heat. *Proceedings of the National Academy of Sciences* 118, e2024792118.

Tyler, J., Entress, R.M., Sun, P., Noonan, D., Sadiq, A.A., 2023. Is flood mitigation funding distributed equitably? evidence from coastal states in the southeastern united states. *Journal of Flood Risk Management* 16, e12886.

Van Migerode, C., Poorthuis, A., Derudder, B., 2024. A spatially-explicit sensitivity analysis of urban definitions: Uncovering implicit assumptions in the degree of urbanisation. *Computers, Environment and Urban Systems* 112, 102149.

Veličković, P., Fedus, W., Hamilton, W.L., Liò, P., Bengio, Y., Hjelm, R.D., 2019. Deep Graph Infomax, in: International Conference on Learning Representations. URL: <https://openreview.net/forum?id=rklz9iAcKQ>.

Wang, C., Wang, Z.H., Yang, J., 2019. Urban water capacity: Irrigation for heat mitigation. *Computers, Environment and Urban Systems* 78, 101397.

Wang, M., Fu, X., Zhang, D., Chen, F., Liu, M., Zhou, S., Su, J., Tan, S.K., 2023. Assessing urban flooding risk in response to climate change and urbanization based on shared socio-economic pathways. *Science of The Total Environment* 880, 163470.

Wang, P., Li, Y., Zhang, Y., 2021. An urban system perspective on urban flood resilience using sem: evidence from nanjing city, china. *Natural hazards* 109, 2575–2599.

Wang, S., Huang, X., Liu, P., Zhang, M., Biljecki, F., Hu, T., Fu, X., Liu, L., Liu, X., Wang, R., et al., 2024. Mapping the landscape and roadmap of geospatial artificial intelligence (geoai) in quantitative human geography: An extensive systematic review. *International Journal of Applied Earth Observation and Geoinformation* 128, 103734.

Wang, Y., Zhu, D., 2024. A hypergraph-based hybrid graph convolutional

network for intracity human activity intensity prediction and geographic relationship interpretation. *Information Fusion* 104, 102149.

Weigand, M., Wurm, M., Dech, S., Taubenböck, H., 2019. Remote sensing in environmental justice research—a review. *ISPRS International Journal of Geo-Information* 8, 20.

Xia, Y., Yabuki, N., Fukuda, T., 2021. Development of a system for assessing the quality of urban street-level greenery using street view images and deep learning. *Urban Forestry & Urban Greening* 59, 126995.

Xu, Y., Hong, T., Zhang, W., Zeng, Z., Wei, M., 2021. Heat Vulnerability Index Development and Mapping. Technical Report. Lawrence Berkeley National Lab.(LBNL), Berkeley, CA (United States).

Yadav, N., Rajendra, K., Awasthi, A., Singh, C., Bhushan, B., 2023. Systematic exploration of heat wave impact on mortality and urban heat island: A review from 2000 to 2022. *Urban Climate* 51, 101622.

Yan, Y., Feng, C.C., Huang, W., Fan, H., Wang, Y.C., Zipf, A., 2020. Volunteered geographic information research in the first decade: a narrative review of selected journal articles in giscience. *International Journal of Geographical Information Science* 34, 1765–1791. doi:10.1080/13658816.2020.1730848.

Yang, Q., Cao, C.F., Li, H.M., Qiu, W.S., Li, W.J., Luo, D., 2023. Is greenery green? an analytical comparison between the planned, visual, and perceived green. *International Journal of Architectural Computing* 21, 498–515. doi:10.1177/14780771231178887.

- Yereseme, A.K., Surendra, H., Kuntoji, G., 2022. Sustainable integrated urban flood management strategies for planning of smart cities: a review. *Sustainable Water Resources Management* 8, 85.
- Yin, C., Peng, N., Li, Y., Shi, Y., Yang, S., Jia, P., 2023. A review on street view observations in support of the sustainable development goals. *International Journal of Applied Earth Observation and Geoinformation* 117, 103205.
- Zhang, F., Salazar-Miranda, A., Duarte, F., Vale, L., Hack, G., Chen, M., Liu, Y., Batty, M., Ratti, C., 2024a. Urban visual intelligence: Studying cities with artificial intelligence and street-level imagery. *Annals of the American Association of Geographers* 114, 876–897.
- Zhang, M., Ma, X., Wang, W., Sheng, J., Cao, J., Cheng, Z., Zhang, X., 2024b. Climate adaptation investments: Short-term shocks and long-term effects of temperature variation on air conditioning adoption. *Sustainable Cities and Society* 108, 105493.
- Zhang, Y., Liu, P., Biljecki, F., 2023. Knowledge and topology: A two layer spatially dependent graph neural networks to identify urban functions with time-series street view image. *ISPRS Journal of Photogrammetry and Remote Sensing* 198, 153–168.
- Zhang, Y., Zheng, X., Helbich, M., Chen, N., Chen, Z., 2022. City2vec: Urban knowledge discovery based on population mobile network. *Sustainable Cities and Society* 85, 104000.

Zhu, A.X., Lu, G., Liu, J., Qin, C.Z., Zhou, C., 2018. Spatial prediction based on third law of geography. *Annals of GIS* 24, 225–240.

Zhu, A.X., Turner, M., 2022. How is the third law of geography different? *Annals of GIS* 28, 57–67.

Zhu, S., Li, D., Huang, G., Chhipi-Shrestha, G., Nahiduzzaman, K.M., Hewage, K., Sadiq, R., 2021. Enhancing urban flood resilience: A holistic framework incorporating historic worst flood to yangtze river delta, china. *International Journal of Disaster Risk Reduction* 61, 102355.